A Mathematical Model for Accessing Liquid Accumulation in Production Tubing: Effect of Tubing Height

Ikputu, Woyengikuro Hilary., Dulu Appah., Emeka Okoro and Solomon Williams

1. Department of Petroleum and Gas Engineering Faculty of Engineering, University of Port Harcourt, Rivers State, Nigeria

Abstract:

Liquid-loading is challenging in mature gas-fields globally. It causes increasing reverse-pressure from increasing liquid-column, thereby significantly affecting production overtime. In this study, a new critical-velocity model was developed for predicting onset of liquid-loading in gas-wells. This was done following the reverse film concept, while incorporating separate pressure drops for both liquid and gaseous phases. Also, influence of production tubing length and liquid-film thickness was equally considered. A comparative analysis of prediction-accuracy of developed-model was also conducted alongside other critical velocity models like Turner et al. (1969), Coleman et al. (1991), Nossier et al. (2000), Li et al. (2001), and Pagou and Wu (2020) models using data from literature. The obtained field data was from 18 vertical gas-wells from Xinjiang North-West gas field in China. The prediction accuracies of critical-velocity models followed the order, Nossier et al. (2000), Turner et al. (1969), Coleman et al. (1991), Li et al. (2001), Pagou and Wu (2020), and developed-model. To increase the prediction accuracy of developed-model, model coefficient adjustments were done by percentage-reduction of developed model coefficient. In the end, the prediction-accuracy of developed-model was tremendously increased by reducing model coefficient.

Keywords: Liquid-loading critical-velocity model, gas-wells, reverse film concept, tubing length

INTRODUCTION

With time, gas-wells experience reduced production as reservoir-pressure depletes. Liquids can cause reduction in production even quicker. Liquid-loading is challenging in mature gas-fields. It comes as an increasing reverse pressure due to increasing liquid-column, which at first will reduce gas well production but overtime, causes a complete stoppage of production (Fan *et al.*, 2018). Therefore, in theory, all gas-wells will encounter liquid-loading at some point. Liquid-loading is liquid-accumulation in wells, causing reduction or in more severe cases, no production. Liquid-loading cause's inefficient recovery and also very expensive remedial solutions is often needed, particularly in wet/retrograde gas-wells (Pagou and Wu, 2020).

Liquid-loading occurs in vertical or deviated wells during production from natural gas reservoirs, and is independent of gas-composition, well temperature or pressure. This is typical in both offshore and onshore production systems and causing simultaneous gas, liquid-hydrocarbons and water flows (Shi *et al.*, 2016). The condensed water vapor is from the fractional water cut and its production is unavoidable. Any effort to prevent it could cause a drastic permeability reduction, which will in-turn cause severe damage to the formation (Belfroid *et al.*, 2008).

Production data analysis for gas wells often must contend with liquid-loading due to inability to concurrently expel produced liquids and gas (Wang *et al.*, 2018). The produced liquids gather to form a hydrostatic pressure in the well. This is very unfavorable to the formation pressure, which is depleting steadily as gas is produced, eventually reducing production to the point where artificial lift must be deployed to lift the liquid load from the well so as to begin gas production again (Guo *et al.*, 2005).

During transient operations, liquid rates can get higher, and will typically show nonlinear responses to the rate change, a phenomenon known as entrainment. Another major source of liquid is when water escapes into the wellbore through a path different from gas (Ardhi, 2016). The water could flow from: casing or parker leaks, behind pipes as a result of cement bond failure, fractures or faults between injectors and producers, natural fracture leading to an aquifer, unfractured wells with or without effective barrier to cross flow, cusping /conning etc (Shi *et al.*, 2016). In any of these cases, whether dry or wet gas-reservoir, is susceptible to early liquid-accumulation (Aboutaleb and Vahid, 2015).

Though liquid-loading is a natural phenomenon, early and massive liquid production could be aggravated by ineffective completion design and poor production practices. Water being the most abundant liquid on earth is very crucial especially when used to boost the reservoir pressure which enhances recovery of hydrocarbon fluids but could also pose technical difficulties when it negatively impacts productive performance and affects the overall operational economics of a field (Joseph and Ajienka, 2010). Unlike oil wells where a large aquifer is of a huge advantage to operators due to its ability to sustain reservoir-pressure, in gas-wells, it poses a very huge challenge to gas-well productivity (Ikoku, 1992).

This is because gas molecules are very light that they would flow without help even at low formation permeability but with water flowing simultaneously with it, the relative permeability is drastically reduced which significantly affects production (Ikoku, 1992). With time, liquid accumulation continues with more condensation from intermediate hydrocarbons and water vapor into production-tubing together with water that directly finds its path. This will cause back-pressure and afterwards kill wells if not properly managed (Nosseir *et al.*, 2000).

The commonest way of predicting onset of liquid-loading is determination of critical-gas velocity through some well-established models. Using this approach, many models have previously been developed (Riza *et al.*, 2016). These critical velocity models are based on continuous film, liquid droplet or reverse film theories of liquid-loading. Some models are quite popular since the parameters needed are readily obtained at the wellhead, which serves a great convenience for field operators (Luo *et al.*, 2014). However, in practice, the existing critical velocity models still fall short in accurately predicting onset of liquid-loading. Sometimes, a coefficient is usually needed to 'adjust' predicted critical-velocities to better fit the situation in fields. This scenario creates need for a better critical velocity model that better predicts liquid-loading.

Therefore, this study focuses on development of a new analytical critical velocity model for predicting liquid-loading.

Concepts of Liquid-Loading in Gas Wells

The first recognizable liquid-loading work was first done by Turner *et al.* (1969). In their study, they proposed two concepts reportedly responsible for liquid-loading. The proposed concepts were continuous-film and entrained liquid-droplet models.
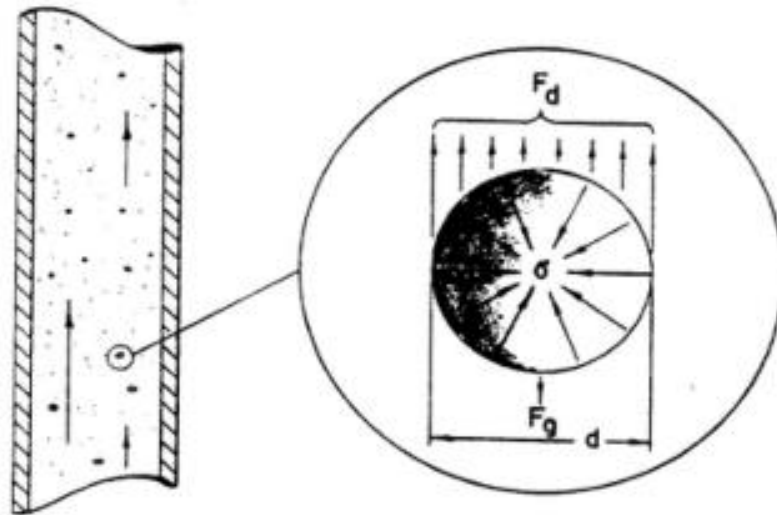
Figure .1 Entrained droplet movement (Turner *et al.*, 1969)

Another popular concept that gained traction later was the reverse film model popularized by Banea (1986). Reverse film model attributes liquid-loading to liquid-film reversal along pipe-walls when the prevalent gas velocity cannot sufficiently carry all liquid. In this concept, liquid-droplets tend to stick to pipe-walls on coming in contact with it. Then, overtime the droplets will coalesce into larger a droplet, which correspondingly increases their dimensions. This continues until droplets are large-enough to flow in a direction opposite the dominant flow direction under gravity. These droplets accumulate overtime at the wellbore causing liquid-loading.
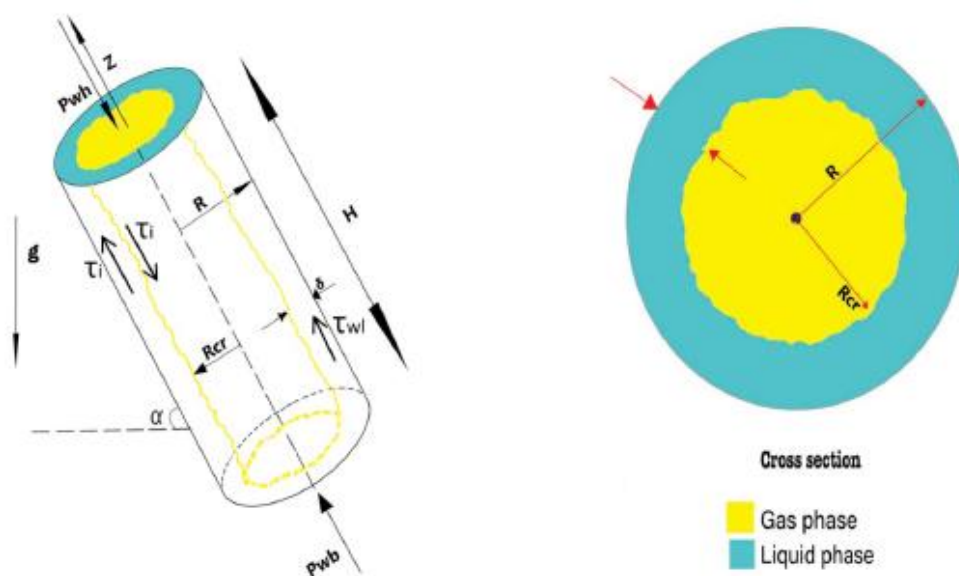
Figure 2 Reverse film flow in annular-flow in gas-wells (Pagou and Wu, 2020)

Following success of Turner *et al.* (1969) model, over time, several scientists have proposed modifications to this model considering various parameters. Pagou and Wu (2020) were able to relate critical-velocity to the liquid-phase viscosity and density, the gravitational forces, gas-liquid in tubing (gas void fraction), and gas-well geometry (tubing diameter, inclination-angle and circumferential angle). Unlike their predecessors, Li *et al.* (2001) supposed liquid-drops transported by gas stream under a high flow rate do have an ellipsoidal shape under the force of pressure difference and high flow-rate, and thereby established their correlation.

Subsequently, Guo *et al.* (2005) built a model dependent on influence of droplets' kinetic energy. Belfroid *et al.* (2008) considered the influence of inclination-angles on inclined gas-wells. Wang *et al.* (2015) considered effect of Weber number on liquid drop and established a new critical gas-velocity. Kumar *et al.* (2017) characterized loading phenomenon using void-fraction. Riza *et al.* (2016) developed a flow regime prediction model that locates loading-point across the pipe. Chen *et al.* (2016) established a model based on liquid-film and gas-core force balances. Okoro *et al.* (2019), while improving the liquid-film model of Chen *et al.* (2016), also considered the volumetric gas-concentration.

However, there appears no research on influence of parameters like height of tubing on liquid-loading. Recently, Wang *et al.* (2018) conducted numerous experiments and found that there is an interconnection between pressure-gradient and gravitational-force, which is partly responsible for the loading phenomenon. But these parameters are sometimes omitted or completely ignored in developing critical velocity models for mathematical convenience. Classical physics indicate that gravitational-force is directly-proportional to height, while pressure-drop in different forms generally accompanies fluid flow in conduits. It becomes imperative that these are incorporated to generate more robust models that truly explains the phenomenon of liquid-loading.

Liquid Unloading Options for Natural Gas Wells
Foaming Agents/Surfactants:
The use of foam produced by surfactants can be effective for gas wells that accumulate liquid at low rates. Foam reduces the density and surface tension of the fluid column, which reduces the critical gas velocity needed to lift fluids to surface and aids liquid removal from the well. Compared to other artificial lift methods, foaming agents are one of the least costly applications for unloading gas wells. Foaming agents work best if the fluid in the well is at least 50 percent water. Surfactants are not effective for natural gas liquids or liquid hydrocarbons.

Surfactants are delivered to the well as soap sticks or as a liquid injected directly into the casing-tubing annulus or down a capillary tubing string. For shallow wells, the surfactant delivery can be as simple as the operator periodically pouring surfactant down the annulus of the well through an open valve. For deep wells, a surfactant injection system requires the installation of surface equipment, as well as regular monitoring. The surface equipment includes a surfactant or 'soap' reservoir, an injection pump, a motor valve with a timer (depending on the installation design), and a power source for the pump. No equipment is required in the well, although foaming agents and velocity tubing may be more effective when used in combination (USEPA, 2011).

Electric pumps can be powered by AC power where available or by solar power to charge batteries. Other pump choices include mechanical pumps that are actuated by the movement of another piece of equipment or pneumatic pumps actuated by gas pressure. Different pump types

have different advantages with respect to reliability, precision, remote operation, simplicity, maintenance frequency, efficiency, and equipment compatibility (USEPA, 2011)

Velocity Tubing:

The velocity at which gas flows through pipe determines the capacity to lift liquids. When the gas flow velocity in a well is not sufficient to move reservoir fluids, the liquids will build up in the well tubing and eventually block gas flow from the reservoir. One option to overcome liquid loading is to install a smaller diameter production tubing or 'velocity tubing'. The cross-sectional area of the conduit through which gas is produced determines the velocity of flow and can be critical for controlling liquid loading. A velocity string reduces the cross-sectional area of flow and increases the flow velocity, achieving liquid removal while limiting blowdowns to the atmosphere (USEPA, 2011).

Usually, it is expected that gas velocity must be at least 5 to 10 ft/sec (300 to 600 ft/min) to effectively remove hydrocarbon liquids from a well, and at least 10 to 20 ft/ sec (600 to 1200 ft/min) to move produced water. Hence, as a rule of thumb, gas flow velocity of 1,000 feet per minute is needed to remove liquid. These figures assume used pipe in good condition with low relative roughness of the pipe wall. The installation of a velocity string is relatively simple and requires calculation of the proper tubing diameter to achieve the required velocity at the inlet and outlet pressures of the tubing. Velocity tubing to facilitate liquid removal can be successfully deployed in low volume gas wells upon initial completion or near the wells upon initial completion or near the end of their productive lives. Candidate wells include marginal gas wells producing less than 60 Mfcd. Installation of velocity tubing requires a well workover rig to remove the existing production tubing and place the smaller diameter tubing string in the well (USEPA, 2011). Coiled tubing may also be used, allowing for easier installation and the application of a greater range of tubing diameters as small as 0.25 inches. Coiled tubing can be applied in wells with lower velocity gas production due to better relative roughness characteristics of the tubing and the absence of pipe joint connections. Studies indicate that seamed coiled tubing provides better lift characteristics due to the elimination of turbulence in the flow stream because the seam acts as a straightening vane.

Plunger Lift with Smart Well Automation:

Plunger lifts are commonly used to lift fluids from gas wells. A plunger lift system is a form of intermittent gas lift that uses gas pressure buildup in the casing-tubing annulus to push a steel plunger and a column of fluid above the plunger up the well tubing to the surface. The operation of a plunger lift system relies on pressure build-up in a gas well during the time that the well is shut-in (not producing). The well shut-in pressure must significantly exceed the sales line pressure in order to lift the plunger and load of accumulated fluid to the surface against the sales line backpressure (USEPA, 2011).

Most plunger systems operate on a fixed time cycle or on a preset differential pressure. Regardless of activation system (manual, fixed time cycle, or preset pressure differential), a valve mechanism and controller at the surface cause gas volume and pressure to build up in the wellbore initiating the plunger release cycle. At this point, the surface valve closes and the plunger drops to the bottom of the well. Once adequate pressure is reached, the surface valve opens and the plunger rises to the surface with the liquid load. Insufficient reservoir energy, or too much fluid build-up can overload a plunger lift. When that occurs, venting the well to the atmosphere (well blowdown) instantaneously reduces the backpressure on the plunger and

usually allows the plunger to return to the surface. Automated control systems optimize plunger lift and well unloading operations to prevent overloading (plunger cannot overcome backpressure and rise to the surface) and underloading (plunger rises to the surface quickly, possibly damaging equipment), therefore reducing or eliminating well venting. Smart automated control systems combine customized control software with standard well control hardware such as remote terminal units (RTUs) and programmable logic controllers (PLCs) to cycle the plunger system and lift fluids out of the tubing. The artificial intelligence component of a smart automation system monitors the tubing and sales line pressures and allows the PLC to learn a well's performance characteristics (such as flow rate and plunger velocity) and to build an inflow performance relationship (IPR) curve for the well. The frequency and duration of the plunger cycle is then modified to optimize well performance. Data analysis combined with wellhead control technology is the key to an effective gas well smart automation system. A smart automation system stores historical well production data allowing the program to learn from experience by monitoring and analyzing wellhead instrument data. The control system relays wellhead instrument data to a central computer, tracks venting times, and reports well problems and high-venting wells, all of which allow custom management of field production (USEPA, 2011).

The components of a smart well automation system that must be installed on each gas well include: remote terminal unit with PLC, tubing and casing transmitters, gas measurement equipment, control valve, and plunger detector. Automated controllers at the wellhead monitor well parameters and adjust plunger cycling. These typically operate on low-voltage, solar batteries. A host system capable of retrieving and presenting data is also required for continuous data logging and remote data transition. Operators configure all controls and send them to the RTU from the host system. Engineering time is needed to customize the control software and optimize the system.

Rod Pumps and Pumping Units:
A downhole positive displacement, reciprocating rod pump with surface pump unit can be deployed in the later stages of a well's life to remove liquids from the wellbore and maximize production until the well is depleted. Pumping units can be installed when there is insufficient reservoir pressure to operate a plunger lift. The units can be manually controlled by the field pumper, or very low volume wells may be operated with a timer. Pumping units not only eliminate the need to vent the well to unload fluids but also extend the productive life of a well. Methane emissions can be further reduced by operating pumping units with electric motors, rather than natural gas-fueled engines. The annual fuel requirement for a typical pumping unit is approximately 1,500 Mcf per unit, of which 0.5 percent is emitted as unburned methane (8 Mcf per unit per year). A well workover rig is required to install the downhole rod pump, rods, and tubing in the well. Field personnel must be trained for rod pump operations and proper maintenance of the surface equipment. Excessive wear of the rods and tubing can be a major expense for rod pump applications where solids are produced or down hole corrosion is a problem. A common problem with reciprocating pumps in gas wells is gas locking of the rod pump valves, which prevents the pump from delivering fluid to the surface at the design rate. The presence of free gas in the subsurface sucker rod pump decreases the volumetric pump efficiency and can prevent the pump from lifting fluid. This is not a problem found in progressive cavity pumps as there are no valves to gas lock (USEPA, 2011).

However, Liquid loading has remained a big challenge and a fundamental issue in gas wells as all gas wells will undergo this phase in their productive life cycle. It is more obvious and severe in aging fields but can also occur in new wells having poor completion designs. When improperly managed or failure to predict its onset accurately, it could lead to not only a tremendous reduction in production but also pose a potential challenge of killing the well. Several studies have developed models to predict the onset of liquid loading. Some of the parameters identified that affect liquid loading include gas density, liquid density, friction factor etc. One of the potential factors that affect critical height is tubing height. However, tubing height has not been considered as a factor in previous studies

Moreso, Liquid loading poses development challenge for both high rate/high pressure gas wells as well as low rate/low pressure gas wells. And depending on tubing string size, surface pressure and density of liquid produced simultaneously with the gas, it could reduce the capacity of a gas well to produce at a required rate over a particular period of time. The implications of a liquid loaded gas well are seen first in reduced revenues due to reduced production rates. Overtime, reduced revenues gradually to zero revenue if the well is not unloaded. The developed model which incorporates tubing height as determining factor will substantially improve understanding of liquid loading in gas wells. This can drastically affect the economics of a given gas project given the effect of delayed profits in a capital-intensive industry like the exploration and production industry. Armed with a better critical velocity model, this problem can be better envisaged and the accompanying costs averted.

In general, loading gas-wells means backflow and liquid-accumulation in wellbores. Some have described this phenomenon (Veeken *et al.*, 2010) as liquid-film that is initially dragged to surface by the gas core along tubing-walls, and later falling and accumulating in wellbores. Some others (Turner *et al.*, 1969; Li *et al.*, 2001; Christiansen *et al.*, 2003; Belfroid *et al.*, 2008) describe it as the flow reversal of droplets initially drained by gas-stream. The flow reversal materializes once reservoir-pressure is insufficient to drain all entrained-liquid to wellhead. When a gas-well experiences loading the backpressure increases, while gas-production decreases; if the accumulation rate is too high, gas-production stops. In the worst-case scenario, operating-company must abandon the wells, and sustain significant economic damages. Therefore, predictions of critical gas-velocity and flow-rate must be made at loading-point to avoid such circumstances and benefit from a long-term, non-loading gas well. If gas-flow rate is smaller than critical-flow rate, the well loads; and, if greater, the well does not load.

Scientists have performed numerous investigations regarding the loading phenomenon, and this has resulted in a division of the scientific community over liquid-loading is explainable using two opposing models: liquid droplet and liquid-film models.

The Liquid Drop Models
The liquid drop model infers that the loading phenomenon originates from the flow reversal or the descent of droplets toward the wellbore. Many scientists have developed models to characterize it. The most widespread model by Turner *et al.* (1969), stipulates that the droplets entrained in high-speed gas stream are spherical. They adopted Hinze (1955) critical Weber-number ranges from 20 to 30 and considers drag-coefficients of 0.44 to be constant in Reynold's number, ranging from 104 to 105. Then, after applying Newton's first law to the ascendant drag force, the ascending buoyant force and the gravity force acting upon the motionless liquid drop, they established critical gas-velocity called Turner model.

Over time, several scientists have proposed modifications to this model. Coleman *et al.* (1991), guided by Turner *et al.* (1969) theory of liquid drop, investigated 56 low-pressure gas-wells and developed a new critical flow-velocity and flow rate correlation. While establishing their model, they validated Turner *et al.* (1969) model, using their field-data, and decried 20% coefficient increase by Turner *et al.* (1969) as unnecessary. Unlike their predecessors, Li *et al.* (2001) supposed that liquid drops transported by gas stream under a high flow rate do, under the force of pressure-difference and high gas-flowrate, have an ellipsoidal shape, and thereby established their correlation. Subsequently, Guo *et al.* (2005) built a model dependent on the influence of the droplets' kinetic energy. Belfroid *et al.* (2008) considered influence of inclination angles on inclined gas-wells, and established a model based on Turner *et al.* (1969) model and the angle correction term of Fiedler and Auracher (2004) which is designed for small diameter tubing. Zhou *et al.* (2010) identified influence of liquid drops amalgamation upon loading-loading and established a critical droplets concentration to determine critical gas-flowrate. Wang *et al.* (2015) considered effect of Weber number on the liquid drop and established a new critical gas-velocity. Li *et al.* (2016), based on Turner *et al.* (1969), developed one to compute critical gas-flowrate in gas-wells. Apart from size and deformation of liquid-drop, their model also accounts for liquid quantities. By authenticating their model with datasets of Turner *et al.* (1969) and Li *et al.* (2001), they found a good match of the computed predictions with the datasets investigated.

Subsequently, Zhang *et al.* (2018) developed dimensionless critical-gas mass-flowrate to identify loading along the entire wellbore. This correlation relies on force balance of liquid-drops in gas-streams. After analysis of the droplet size in the gas stream, they found that largest liquid-sizes rely on the liquid drop breakup in co-current annular-flow and the liquid drop drainage in churn-annular flow. Furthermore, they found that, as gas flow-rate increases and the tubing diameter decreases, dimensionless critical mass flow rate decreases, thus reducing loading. Additionally, they also found that loading could be prevented by lowering surface-tension.

Although liquid-droplet model is recognized and appreciated by the scientific community for its simple design, some scientists have failed to find visual proof, in experiments or gas-wells, that corroborates the conception of liquid-droplets as causing liquid-loading. Therefore, Alamu *et al.* (2012) conducted some experiments and proved that the proportion of entrained-droplets is fewer than that liquid-film during change in flow regime (annular to churn flow regime). Wang (2014) conducted some experiments on two-phase flow-regimes (gas-liquid) in the deviated and horizontal tubes. They discovered liquid-drop flows to a certain point and then arrive at tubing-wall to amalgamate into liquid-films.

The Liquid Film Models
Unlike the liquid drop model, liquid-film model infers that the liquid film must flow primarily upward along tubing-wall. The moment it starts to flow downward is the loading point. Several scientists established models to determine initial loading point based on liquid film reversal theory. Wallis (1969) established a model to compute sufficient gas velocity needed to entrain all the liquid to wellhead. Barnea *et al.* (1982), after multiple investigations, found down flow of liquids occurs at a gas void fraction equal to 0.65. Later, a model based on change of flow regime proposed by Barnea (1986) showed unsteadiness of liquid-film and the blockage of gas-core generates the annular to slug/churn flow regime conversion. He developed his model based on the film-thickness is uniform inside the inclined pipe, and neglected occurrence of droplets in gas-stream. Usui and Sato (1989), Jiang and Rezkallah (1993), and Kumar *et al.* (2017) characterized the loading phenomenon according to void-fraction. Through multiple

experiments, they found that loading manifests when gas void-fraction ranges from 0.8 to 0.9. Based on those experiments, they established correlations to compute gas void-fraction.

Later, Godbole (2009) and Bhagwat (2011) followed their example and used gas void-fraction to predict loading. After performing several experiments, they determined that the gas void fraction ranges from 0.7 to 1 at the loading onset, and then established their correlations. Van't Westende *et al.* (2007), after conducting air-water flow measurement experimentations on liquid-drop size and velocity in a 12 m long tubing, with a 0.05 m inner diameter, concluded loading starts when film and gas flow are moving in directions that are counter-current. Veeken *et al.* (2010) confirmed those observations while modeling loading via transient-multiphase flow-simulator "OLGA". Later, Van't Westende (2008), Guner (2012), Alsaadi (2013), and Li *et al.* (2014), on the basis of the Barnea (1986, 1987) model, established a mechanistic-model to forecast loading in inclined wells.

After conducting numerous experiments, they found that from 0° (corresponding to horizontal) to 60°, film thickness increases gradually, until reaching its maximum value at nearly 60°, as does critical-gas flowrate; then, from 60° to 90°, film-thickness at lower section of pipe reduces rapidly, as does critical-gas flowrate. Thus, they established correlations characterizing the non-uniform film-thickness on the basis of the inclination angle and the position of the pipe circumference. Additionally, Li *et al.* (2014); Luo *et al.* (2014); Fan *et al.* (2018) through several experiments, identified an interdependency between film-gravity and the pressure gradient that has a significant influence on loading. After numerous experimentations on liquid-film reversal, Waltrich *et al.* (2015) concluded that Wallis (1969) model is accurate enough to predict loading.

Chen *et al.* (2015) investigated the inclined pipe dynamic wave characteristics before the liquid reversal happens and flow-regime transition when it happens by using the computational fluid dynamic (CFD) method. The validation of their model shows their results agree well with the laboratory dataset collected. Their results show smaller surface tension will shred the interfacial waves into minuscule droplets, which will expand into the mist flow. Further analysis showed increase of liquid viscosity would cause denser liquid film holdup which would be more favourable to develop a slug flow.

Riza *et al.* (2016), after assuming loading initiates when annular-flow changes to a slug flow regime, developed a flow regime prediction model that locates loading-point across the pipe. They found loading occurs at wellbore, rather than at top. Chen *et al.* (2016) established a model based on liquid-film and gas-core force balances. Final model combined Turner et al. model and a correction term for every inclination-angle.

Pagan and Waltrich (2016) gave a model for initiation of loading in transient flows. Their model is based on nodal-analysis technique. Rather than implementing the usual critical-velocity or minimum-pressure notion, they modified tubing-performance-relationship. This modification facilitated the simple implementation of nodal analysis to forecast liquid-loading inception and time frame necessary for production to stop after the beginning of loading. After validating their model with field-dataset, they found that their prediction-results matched well with field-data.

Joseph and Hicks (2018) proposed a dynamic-simulation method to investigate liquid-loading in gas-wells experiencing mist-flow. They considered the two-component gas-liquid two-phase flow. Then, they implemented the coupled hydrodynamic and thermodynamic model, with

constitutive-equations that integrate Peng-Robinson EoS and convex-hull algorithm. They obtained a correlation that assesses loading by determining liquid-density distribution in the pipe via flow-variables. They validated their model by comparing phase densities they computed to results from NIST RefProp, which showed good-match between the two results.

Tang *et al.* (2018) gave a fully-implicit coupled wellbore/reservoir model to delineate the transitional flow in horizontal gas-wells experiencing loading. Relying on control-volume finite-difference method, they completely coupled a wellbore model with simulator designed by themselves. They proposed an adjusted drift-flux model, which can predict variation in flow-regime in horizontal and vertical gas wells. Then, they integrated this latter to coupled wellbore/reservoir simulator to illustrate two-phase flow in horizontal-wellbores. After validation of their model, they noted amended drift-flux correlation, aside from matching the production prediction and wellbore pressure of commercial simulator, also forecasts the inconstant liquid production generated by flow-regime changes.

Moreover, a parametric analysis showed that increase in inflow zones decreases flow-regime's variation time. Further analysis demonstrated that simultaneously increasing the tubing-head pressure and reducing the reservoir depth led to an increase in flow-regime transition time. Additionally, while implementing their model at an artificial field scale, their model was able to predict 23 more days of gas-production than a commercial-simulator. Later, Wang *et al.* (2018) conducted numerous experiments and found an interconnection between pressure-gradient and gravitational-force, which is partly responsible for loading phenomenon. Given those findings and after investigating the film thickness at the lower end, and liquid-gas interfacial friction-factor, they developed a loading mechanism for all pipes.

Based on film force balance at bottom of deviated and vertical tubing, they established an analytical model to evaluate loading, which considers influences of variations in fluids properties. Liu *et al.* (2018), after several investigations, also found loading was firmly related to film-gravity. They assumed film-thickness to be uniform at any inclination angle (0°–90° corresponding to vertical well), and then by implementing Navier-Stokes liquid-film equations only, derived a critical gas velocity correlation.

Then, they associated their critical velocity expression with the Fiedler and Auracher (2004) well inclination angle model to predict loading in inclined wells. It is noteworthy that the Liu *et al.* (2018) correlation is exclusively a function of film parameters, tubing-diameter, and inclination-angle.

Tang *et al.* (2019) also developed a fully-implicitly coupled wellbore/reservoir model based on both the momentum and mass balances. The developed model investigates influences of liquid-loading on horizontal-wells in low-permeability gas-reservoirs. Furthermore, it also studies reservoir dynamics and wellbore after the occurrence of loading. After validation of their model, they found that horizontal gas-wells in low-permeability reservoirs could endure natural cyclic-production after the occurrence of loading. To mitigate this latter, they suggested the implementation of both uniform-stimulation and hydraulic-fracturing method. Choosing between the two methods is because they will lower the initial pressure-difference between near-wellbore and wellbore reservoir when the loading phenomenon takes place.

Later, Adaze *et al.* (2019) performed a CFD-simulation to the falling film phenomenon in annular-flow in a vertical-pipe of 76.2 mm by performing 2D axisymmetric numerical-simulations via ANSYS. Water and air were the working-fluids, and the tubing was 3 m long. After authentication with dataset from literature, results from their model match well the laboratory results. Moreover, a considerable fluctuation of the shear stress due to viscous sub-layer was observed at proximity of tubing-wall where liquid is more significant, then reduced progressively towards tubing center. Additionally, they also concluded that transfer of mass at the gas-liquid boundary might also have impact on shear stress and its time-space fluctuations. Afterwards, Okoro *et al.* (2019) developed model to predict loading by modifying the Chen *et al.* (2016) model accounting for non-uniform film-thickness and integrating a new interfacial friction-factor more representative of large film-thickness. Upon validation with a deviated gas field dataset, their model obtained better prediction accuracy than the Chen *et al.* (2016) model.

Finally, Rastogi *et al.* (2019), through laboratory experimentations, demonstrated liquid-film reversal causes loading. Therefore, they proposed a model based on mechanism triggering liquid-film reversal. Moreover, they developed a model to compute film-thickness around tubing-wall. They obtained a model that reflects well influences of liquid flow-rate, densities and viscosities, inclination-angle and tubing-diameter on critical-gas flowrate. The authentication of their model shows it outperforms all others. Throughout gas-production, gas-stream is driving-force while draining the liquids.

Several scientists showed that gradual decrease of gas-flowrate in annular-flow changes into an annular wavy, with uniform film-thickness in vertical-wells (Wallis, 1969; Barnea, 1986, 1987; Guner *et al.*, 2015; Liu *et al.*, 2018) and non-uniform film-thickness in inclined wells (Guner, 2012; Alsaadi, 2013; Li *et al.*, 2014; Luo *et al.*, 2014; Shekhar *et al.*, 2017). Ultimately, as superficial gas-velocity continues to decrease, wave height continues to increase until they form a gas-core blockage, thereby initiating the loading phenomenon.

Pagou and Wu (2020) also developed a new model for liquid-loading. From their review of literature, they found liquid-flowrate is often far smaller than gas-flow rate. So, they reasoned it more logical to relate critical-gas flowrate model to flowing gas-rate rather than to film-flow rate. Furthermore, they also thought it more reasonable to relate it to uniform film-thickness (for vertical wells), non-uniform film-thickness (inclined wells), pressure-gradient, and gas-phase viscosity and density.

Additionally, they were able to relate critical-velocity to the liquid-phase viscosity and density, the gravitational forces, gas-liquid in the tubing (gas void fraction), and gas-well geometry (tubing diameter, inclination angle and circumferential angle). They developed their model, which predicts and identifies liquid-loading in gas wells through two steps. The first step consisted of establishing the correlation that quantifies the gas-liquid amount in gas-well (gas void fraction) through modification of Barnea (1986) model, thereby predicting the loading and unloading flow regime. Then, they developed the Hagen-Poiseuille equations, with gravity being considered for the gas-phase and liquid-phase. Then, they associated flowrate correlation to the Luo *et al.* (2014) circumferential angle to consider non-uniform film-thickness in inclined gas wells. Consequently, their new model related loading directly to liquid-film, flowing gas-core influential parameters, the gas-liquid amount (gas void fraction), the tubing inner diameter, inclination-angle, and circumferential-angle. Moreover, it also related the loading phenomenon to the flowing gas rate, pressure-gradient, gravitational-forces, uniform film-thickness (for

vertical wells), the non-uniform film thickness (for inclined wells only), and changes in both fluids' properties (densities and viscosities). They collected field data from vertical wells like the Xinjiang North-West gas field, Turner *et al.* (1969) dataset, and Coleman *et al.* (1991) data set and inclined gas wells data set like the Chuanxi and Daniudi gas field published by Gao (2012) and Veeken *et al.* (2010) data set to authenticate their proposed model.

Vieira *et al.* (2021) introduced a new model for predicting liquid loading onset, based on the reversal of a non-uniform liquid film. The momentum balance equation for annular flow in the proposed model was expressed as a function of liquid holdup instead of liquid thickness. The model employs auxiliary correlations to obtain liquid holdup and an interfacial friction factor, developed from literature data. The accuracy of their proposed model was quantified by comparing laboratory data from their work and field datasets from previous studies, with the predictions of existing models.

The proposed model was able to successfully reproduce the experimental data and field data, and gives the highest prediction accuracy and the lowest average error when compared with existing models. The applicability of the auxiliary correlations shows that their model is restricted to upward pipe inclinations of 30°–90° from the horizontal, liquid viscosities of 1.1 cP and 0.018 cP, and superficial velocities of gas of 3–60 m/s and of liquid of 0.01–0.2 m/s. Their results also showed that the model exhibits poor performance when applied to pipe inclinations lower than 30° from the horizontal.

Prediction Models for Critical Velocity
Turner's Model:
Turner *et al.* (1969) proposed two physical models for the removal of gas well liquids. The models are based on: (1) the liquid film movement along the walls of the pipe and (2) the liquid droplets entrained in the high velocity gas core. They used field data to validate each of the models and concluded that the entrained droplet model could better predict the minimum rate required to lift liquids from gas wells.

This is because the film model does not provide a clear definition between adequate and inadequate rates as satisfied by the entrained droplet model when it is compared with field data. A flow rate is determined adequate if the observed rate is higher than what the model predicts and inadequate if otherwise. Again, the film model indicates that the minimum lift velocity depends upon the gas-liquid ratio while no such dependence exists in the range of liquid production associated with field data from most of the gas wells (1 - 130 bbl/MMSCF). The theoretical equation for critical velocity V_t to lift a liquid drop is given below in field units and in terms of pressure.

$$V_{c,w} = \frac{5.304 \, (67-0.0031P)^{1/4}}{\sqrt{0.0031P}} \qquad (1)$$

Where
$V_{c,w}$ = critical velocity (ft/s)
P = pressure (psia)

Coleman's Model:
Using the Turner model but validating with field data of lower reservoir and wellhead flowing pressures all below approximately 500 psia, Coleman *et al.* (1991) was convinced that a better prediction could be achieved without a 20% upward adjustment to fit field data with the following expressions in field units and in terms of pressure:

$$V_{c,w} = \frac{4.434 \, (67-0.0031P)^{1/4}}{\sqrt{0.0031P}} \qquad (2)$$

Where
$V_{c,w}$ = critical velocity (ft/s)
P = pressure (psia)

Li's Model:
Li *et al.* (2001) in their research posited that Turner and Coleman's models did not consider deformation of the free-falling liquid droplet in a gas medium. They contended that as a liquid droplet is entrained in a high- velocity gas stream, a pressure difference exists between the fore and aft portions of the droplet. The droplet is deformed under the applied force and its shape changes from spherical to a convex bean with unequal sides (flat). They therefore, proposed the following model represented here in S.I. units:

$$V_{c,w} = \frac{2.5 \, \sigma^{1/4}(\rho_l-\rho_g)^{1/4}}{\sqrt{\rho_g}} \qquad (3)$$

Where
$V_{c,w}$ = critical velocity (m/s)
σ = interfacial tension (N/m)
ρ_g = natural gas density (Kg/m³)
ρ_l = liquid density (Kg/m³)

Nossier's Model:
Nosseir *et al.* (2000) focused their studies on the impact of flow regimes and changes in flow conditions on gas well loading. They followed the path of Turner droplet model but, they made a difference from Turner model by considering the impact of flow regimes on the drag coefficient (C). Turner model takes the value of C_d to be 0.44 under laminar, transition and turbulent flow regimes, which in turn determine the expression of the drag force and hence critical velocity equations. On comparing Nossier observed that Turner model values were not matching with the real data for highly turbulent flow regime. Dealing with this deviation, Nossier found out the reason to be the change in value of C_d for this regime from 0.44 to 0.2. For

$$V_{c,w} = \frac{14.6 \, \sigma^{0.35}(\rho_l-\rho_g)^{0.21}}{\mu_g^{0.134}\rho_g^{0.426}} \qquad (4)$$

Where
$V_{c,w}$ = critical velocity (ft/s)
σ = interfacial tension (lbf/ft)
ρ_g = natural gas density (Kg/m³)
ρ_l = liquid density (Kg/m³)
μ_g = viscosity (cP)

Nossier derived the critical flow equations by assuming C_d value of 0.44 for Reynolds number (R_e) 2×10^5 to 10^6 and for Re value greater than 10^6 he took the C_d value to be 0.2. Again, the critical velocity equation for highly turbulent flow regime is given in field units as:

$$V_{c,w} = \frac{21.3 \, \sigma^{0.25}(\rho_l - \rho_g)^{0.25}}{\rho_g^{0.5}}$$ (5)

Where
$V_{c,w}$ = critical velocity (ft/s)
σ = interfacial tension (lbf/ft)
ρ_g = natural gas density (Kg/m³)
ρ_l = liquid density (Kg/m³)

Coefficient of Drag

Multiphase flow involving suspensions of liquid droplets or gas bubbles are frequently encountered in many industrial processes including oil and gas production. The ability of fluids in horizontal motion to suspend the droplets depends mainly on the balance of two actions: gravity, which causes the droplets to fall or settle in the fluid, and an upward diffusion, caused by a concentration gradient which in turn is created by gravity. The droplet movement thus, depends on their properties such as solids density, particle size and particle shape. The gravitational force causing the particle to rise or fall can be defined as (Govier and Aziz, 1972):

$$F_G = \frac{\pi}{6} d^3 g (\rho_l - \rho_g)$$ (6)

The rise or fall of the droplet in the fluid results in a lift and drag force where this force may be expressed as:

$$D = \frac{\pi}{8} d^2 \rho_g C_d u^2$$ (7)

Where ρ_l is the liquid density, ρ_g is the gas density, d is the diameter, m, g is the acceleration due to gravity, C_d is the drag coefficient and v is the rise or fall velocity. The drag force arises from pressure and viscous stresses applied to the particle surface and resist the relative fluid velocity v. The magnitude of drag is primarily dictated by the particle's Reynolds number, R_e, defined as:

$$R_e = 1488 \frac{\rho u d}{\mu}$$ (8)

Where u is the fluid velocity (ft/s), d is the particle diameter (ft), ρ is fluid density (lbm/ft³) and μ is the fluid viscosity (cp). The drag coefficient is a very important hydrodynamic parameter involved in the modelling and design of multiphase processes, especially when entrained with droplets.

The definition of the drag force on a droplet in a fluid flow generally involves the understanding of the relationship between the drag coefficient C_d and particle's Reynolds number, R_e. The drag coefficient represents the fraction of the kinetic energy of the settling velocity that is used to overcome the drag force on the droplet, while the Reynolds number is a ratio between the inertial and viscous forces of a fluid. As the droplet size or flow velocity increases for a given kinematic viscosity, so does the Reynolds number, and the character of flow changes. For very small

Reynolds numbers, Stokes proposed an analytical solution of drag coefficient by solving the general differential equation of Navier–Stokes (Bello and Idigbe, 2015).

$$C_d = \frac{24}{R_e} \tag{9}$$

An analytical attempt to extend the range of approximation for the drag coefficient beyond Stokes flow was proposed by some authors by including the inertia terms in the solution of Navier–Stokes. Several correlations for drag coefficient have been proposed over a wide range of Reynolds number in the literature. A number of empirical and semi empirical C_d–$R_e$relationships have been proposed.

Cheng (2009) proposed a drag coefficient model which has greater applicability when compared with other models evaluated. These other models can only be used for limited Reynolds numbers and even those applicable for wider range of R_e, may involve tedious application procedure. The model proposed by Cheng given below, despite its simple form, gives the best approximation of experimental data for R_e, from Stoke's regime to about 2×10^5 (Bello and Idigbe, 2015).

$$C_d = \frac{24}{R_e}(1 + 0.27R_e)^{0.43} + 0.47[1 - exp(-0.04R_e^{0.38})] \tag{10}$$

This drag coefficient C_d is predicted from two terms. The first term on the RHS can be considered as an extended Stokes' law, applicable approximately for $R_e < 100$; and the second term is an exponential function accounting for slight deviations from the Newton's law for high R_e. The sum of the two terms is used to predict drag coefficient for any R_e over the entire regime.

Ruiquing and Huiqun (2017) also proposed a cubic equation representing the relationship between drag coefficient and Reynolds number for both transition and turbulence flow regimes. As known by the standard experimental drag curve, drag coefficient fluctuates heavily under the condition of transition flow and turbulence flow ($2 \times 10^5 \leq R_e \leq 10^6$). It is obviously unreasonable to take drag coefficient as a fixed value. Thus, they used SPSS to conduct nonlinear fitting of the experimental data in transition flow and turbulence flow (Ruiquing and Huiqun, 2017).
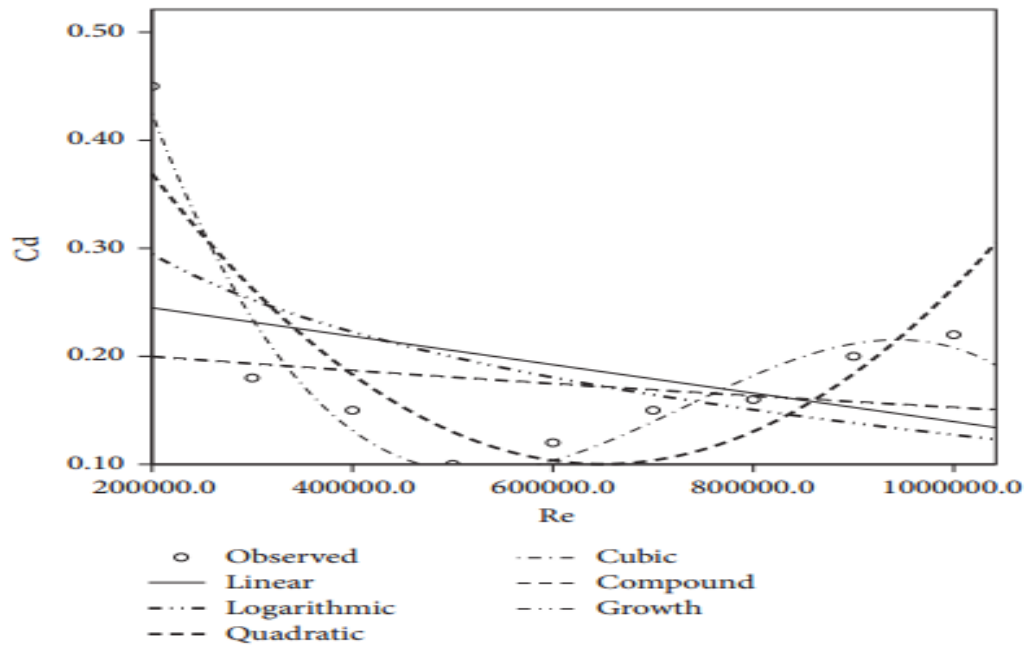
Figure 3: Showing non-linear fitting of experimental data of drag coefficient and Reynold's number for transition and turbulence flow regimes (Ruiquing and Huiqun, 2017)

As can be seen from Figure 2.1, which shows that the cubic fitting of this model is better than others, indicating that regression model fitting results are good. Therefore, the cubic model in transition flow and turbulence flow was taken as presented below:

$$C_d = -3.3316 \times 10^{-18} R_e^3 + 7.3 \times 10^{-12} R_e^2 - 4.918 \times 10^{-6} R_e + 1.143 \quad (11)$$

Gas Well Deliquefaction Techniques

There is no one size fits all solution for wells with liquid loading. The optimal solution depends on the particular conditions of the well. Methods like downsizing of production tubing inner diameter (ID), reduction of the density of the production liquids, cyclic shut-in control, and plunger lift rely on the internal energy of the well. On the other hand, the applications of artificial lift methods such as gas lift and production pumps rely on the introduction of external energy. Contrary to some other studies, the current study does not recognize compression as a liquid lifting technique. Compression is considered a must-have in gas wells (in late-life) and thus thought to be indispensable.

When the produced gas is directed to the suction of the compressor, gas pressure is increased as much as the compression ratio before the gas is injected into the pipeline. This allows lowering of the WHP much below the pipeline pressure. Lowering the WHP (and accordingly BHP) causes considerable increments in drawdown pressure, hence in gas flow rate. Increased rate (gas velocity) helps unload the wellbore much easier. In addition, when the abandonment pressure of the well is reduced, ultimate recovery is increased considerably. Contrary to their relatively high initial investment requirement, compressors are almost always necessary to get the most out of gas wells and they can be used in several wells within their economic life.

Deliquification (dewatering) is also a necessity in most unconventional gas wells to initiate production. With the growth of unconventional plays, the topic of deliquification will continue to be of great importance. For example, in coalbed methane (CBM) wells, initially water is produced

to reduce reservoir pressure and leads to gas desorption from the organic matter, which flows into the wellbore. Likewise, methane hydrate (gas hydrate) formations need pressure reduction, which can be provided by the production of free formation water. Production of this free water breaks the hydrate equilibrium condition (hydrate cage structure) and methane is produced. Most shale gas wells suffer from liquid loading during the initial flow-back phase (producing the fracturing fluid) and sometimes during the production phase (according to formation characteristics).

Several authors have extensively reviewed deliquification methodologies and provided screening criteria or decision-making tools. The parameters which determine the deliquification method selection criteria are very easy-to-monitor production parameters such as liquid rate, liquid type, WHP, and GLR. Other well/wellbore design parameters such as well inclination, tubing ID/uniformity, well/perforation depth and other bottom hole equipment (subsurface safety valves (SSSV), mandrels) also have bearing on the chosen deliquification method.

When screening the unloading techniques, both technical and economic feasibility should be considered

MATERIALS AND METHODS

Research Design
a) The first step taken in carrying out this research was to conduct extensive review of literature to identify existing gaps.
b) Following the identified gaps, a new analytical critical-velocity model was developed based on reverse film concept.
c) Meanwhile, the evaluation of the model accuracy was done using 18 gas wells data acquired from North-West Xinjiang gas-field as gotten from Pagou and Wu (2020).
d) Furthermore, comparisons of the accuracy results were carried against critical-velocities obtained using Turner *et al.* (1969), Coleman *et al.* (1991), Nossier *et al.* (2000), Li *et al.* (2001), and Pagou and Wu (2020) models.

Model Development
The configuration of the annular flow locates the liquid between the inner tubing wall and the gas stream. The model developed is founded on fluid-film reversal. It is assumed that the change of flow-regime from annular (gas core surrounded by liquid-film) to churn or slug generates loading. For ensuing treatment, following assumptions were made:
a) Flow of liquid-film is gravity-driven
b) Liquid-film flow is steady and considered fully developed laminar
c) Liquids are Newtonian and incompressible
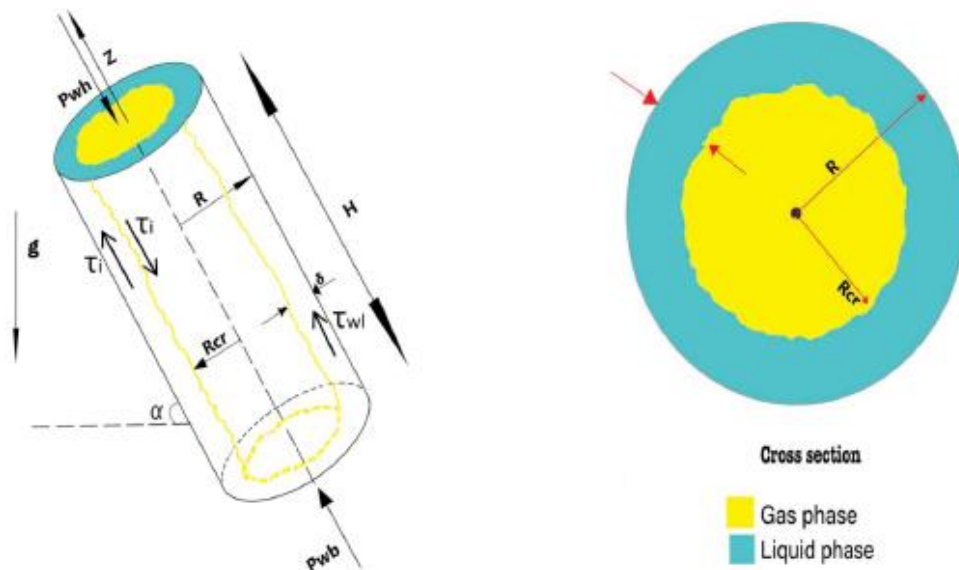d) Film-thickness is uniform all-around circumference zone

Figure 4 Reverse film flow in annular flow in gas wells (Pagou and Wu, 2020)

Occurrence of Bubbles is Negligible

Carrying out a force-balance on gas-core and surrounding liquid moving in production tubing in Figure 3.1 experiencing annular flow (Barnea, 1986),

$$-V_c \left(\frac{dP}{dL}\right)_c - \tau_i S_i - V_c \frac{\rho_g g}{g_c} = 0 \qquad (12)$$

$$-V_f \left(\frac{dP}{dL}\right)_f + \tau_i S_i - \tau_{wi} S_l - V_f \frac{\rho_l g}{g_c} = 0 \qquad (13)$$

Where

V_c = gas core volume (ft³)

$\left(\frac{dP}{dL}\right)_c$ = gas core pressure drop (psf)

S_i = gas core surface area (ft²)

ρ_g = gas density (lbm/ft³)

V_f = liquid film volume (ft³)

$\left(\frac{dP}{dL}\right)_f$ = liquid film pressure drop (psf)

S_l = liquid film surface area (ft²)

ρ_l = liquid film density (lbm/ft³)

τ_i = interfacial shear-stress (lbf/ft²)

τ_{wi} = liquid film wall shear-stress (lbf/ft²)

g = acceleration due to gravity (32.17 ft/s²)

g_c = conversion factor (32.17 lbm-ft/lbf-s²)

Subtracting Equ. (1.2) from Equ. (13),

$$-V_c \left(\frac{dP}{dL}\right)_c - \left\{-V_f \left(\frac{dP}{dL}\right)_f\right\} - \tau_i S_i - \tau_i S_i - (-\tau_{wi} S_l) - V_c \frac{\rho_g g}{g_c} - \left\{-V_f \frac{\rho_l g}{g_c}\right\} = 0$$

$$(14)$$

Simplifying,

$$-V_c \left(\frac{dP}{dL}\right)_c + V_f \left(\frac{dP}{dL}\right)_f - 2\tau_i S_i + \tau_{wi} S_l - V_c \frac{\rho_g g}{g_c} + V_f \frac{\rho_l g}{g_c} = 0 \qquad (15)$$

Rearranging,

$$V_f \left(\frac{dP}{dL}\right)_f - V_c \left(\frac{dP}{dL}\right)_c - 2\tau_i S_i + \tau_{wi} S_l + V_f \frac{\rho_l g}{g_c} - V_c \frac{\rho_g g}{g_c} \qquad (16)$$

But,

$$V_f = (1 - \epsilon) \frac{\pi D^2}{4} L \qquad (17)$$

$$V_c = \epsilon \frac{\pi D^2}{4} L \qquad (18)$$

Where
ϵ = volumetric gas concentration (-)
D = tubing diameter (ft)
L = tubing length (ft)
Substituting Equ. (16) and Equ. (17) into Equ. (15), we have

$$(1 - \epsilon) \frac{\pi D^2}{4} L \left(\frac{dP}{dL}\right)_f - \epsilon \frac{\pi D^2}{4} L \left(\frac{dP}{dL}\right)_c - 2\tau_i S_i + \tau_{wi} S_l + (1 - \epsilon) \frac{\pi D^2}{4} L \frac{\rho_l g}{g_c} - \epsilon \frac{\pi D^2}{4} L \frac{\rho_g g}{g_c}$$
$$(19)$$

When fluid-film obstructs gas-stream, gas-core energy is less than liquid-film gravity-force. At that moment, not only does frictional pressure gradient becomes negligible compared to film gravity force, but also liquid-film wall shear stress vanishes. Here, pressure-drop is expressed as (Pagou and Wu, 2020):

$$\left(\frac{dP}{dL}\right)_c = \frac{\rho_g g}{g_c} \qquad (20)$$

$$\left(\frac{dP}{dL}\right)_f = \frac{\rho_l g}{g_c} \qquad (21)$$

Substituting Equ. (20) and Equ. (21) into Equ. (19), we have

$$(1 - \epsilon) \frac{\pi D^2}{4} L \frac{\rho_l g}{g_c} - \epsilon \frac{\pi D^2}{4} L \frac{\rho_g g}{g_c} - 2\tau_i S_i + \tau_{wi} S_l + (1 - \epsilon) \frac{\pi D^2}{4} L \frac{\rho_l g}{g_c} - \epsilon \frac{\pi D^2}{4} L \frac{\rho_g g}{g_c} = 0$$
$$(22)$$

Collecting like terms,

$$2(1 - \epsilon) \frac{\pi D^2}{4} L \frac{\rho_l g}{g_c} - 2\epsilon \frac{\pi D^2}{4} L \frac{\rho_g g}{g_c} - 2\tau_i S_i + \tau_{wi} S_l = 0 \qquad (23)$$

$$\frac{2\pi D^2 L g}{4 g_c} \{(1 - \epsilon)\rho_l - \epsilon \rho_g\} - 2\tau_i S_i + \tau_{wi} S_l = 0 \qquad (24)$$

Recall, when fluid-film obstructs gas- stream (Pagou and Wu, 2020),

$$\tau_{wi} = 0 \qquad (25)$$

Also, gas-core and liquid-film surface areas are,

$$S_i = \frac{\pi D_{cr}^2}{4} \tag{26}$$

$$S_l = \frac{\pi D^2}{4} \tag{27}$$

$$\tau_i = \frac{1}{2} f_i \rho_g \frac{v_{cr}^2}{\epsilon^2} \tag{28}$$

Where
D_{cr} = diameter of gas core/critical diameter (ft)
f_i = interfacial friction factor (-)
v_{cr} = critical velocity (ft/s)

Substituting Equ. (26)-(27) into Equ. (28),

$$\frac{2\pi D^2 Lg}{4g_c}\left\{(1-\epsilon)\rho_l - \epsilon\rho_g\right\} - 2\left\{\frac{1}{2} f_i \rho_g \frac{v_{cr}^2}{\epsilon^2}\right\}\frac{\pi D_{cr}^2}{4} = 0 \tag{29}$$

For inclined production tubings, Equ. (29) can equally be expressed as

$$\frac{2\pi D^2 Lg}{4g_c}\left\{(1-\epsilon)\rho_l - \epsilon\rho_g\right\}sin\alpha - \left\{f_i \rho_g \frac{v_{cr}^2}{\epsilon^2}\right\}\frac{\pi D_{cr}^2}{4} = 0 \tag{30}$$

$$\frac{\pi D^2 Lg}{2g_c}\left\{(1-\epsilon)\rho_l - \epsilon\rho_g\right\}sin\alpha = \left\{f_i \rho_g \frac{v_{cr}^2}{\epsilon^2}\right\}\frac{\pi D_{cr}^2}{4} \tag{31}$$

Making v_{cr}^2 the subject,

$$v_{cr}^2 = \frac{2\epsilon^2 D^2 Lg}{g_c D_{cr}^2 f_i \rho_g}\left\{(1-\epsilon)\rho_l - \epsilon\rho_g\right\}sin\alpha \tag{32}$$

However, the volumetric gas-concentration is also expressable as,

$$\epsilon = \frac{R_{cr}}{R} = \frac{D_{cr}}{D} \tag{33}$$

And

$$Z = Lsin\alpha \tag{34}$$

So that,

$$sin\alpha = \frac{Z}{L} \tag{35}$$

Where
Z = true vertical tubing height
Substituting Equ. (33) and Equ. (3.4) into Equ. (32),

$$v_{cr}^2 = \frac{2gZ}{g_c f_i \rho_g}\left\{(1-\epsilon)\rho_l - \epsilon\rho_g\right\} \tag{36}$$

Taking square root of both sides,

$$v_{cr} = \sqrt{\frac{2gZ}{g_c f_i \rho_g}\left\{(1-\epsilon)\rho_l - \epsilon\rho_g\right\}} \tag{37}$$
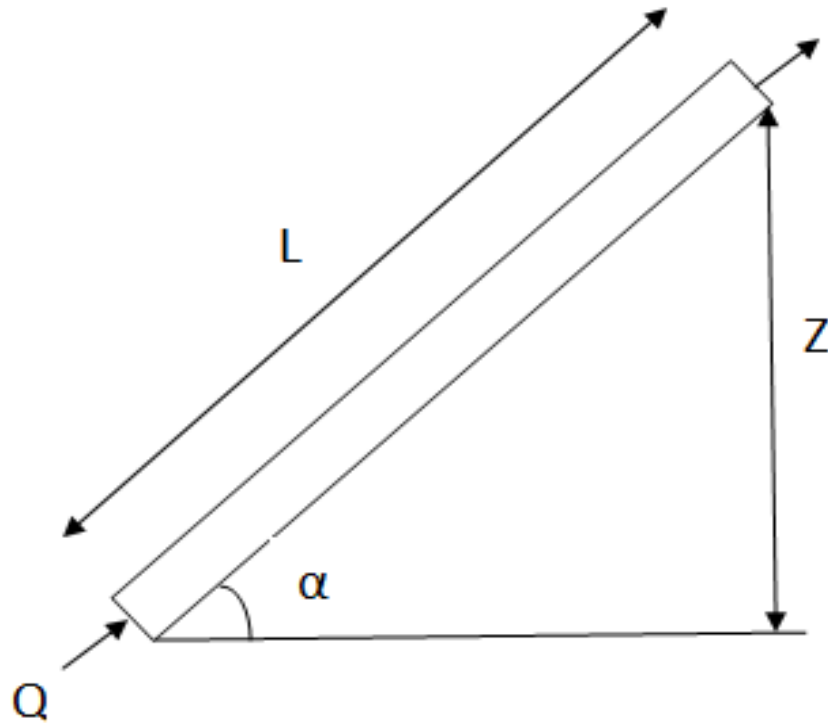
Figure 5 An inclined gas well production tubing showing true vertical tubing height (Ikoku, 1992)

Interfacial Friction Factor
The interfacial friction factor correlated by Fore *et al.* (2000) is ratified for calculation consistency and is:

$$f_i = 0.005 \left[1 + 300 \left\{1 + \frac{17500}{Re_g} \frac{\delta}{D} - 0.0015\right\}\right] \tag{36}$$

Hewitt and Nicholls (1969) researches on the annular two-phase flow measurement of the liquid film width and found wave heights 4 to 6 times higher than average film-width (δ), and proposed:

$$1 - \epsilon = 4\frac{\delta}{D}\left(1 - \frac{\delta}{D}\right) \tag{37}$$

On rearranging,

$$4\left(\frac{\delta}{D}\right)^2 - 4\left(\frac{\delta}{D}\right) + (1 - \epsilon) = 0 \tag{38}$$

Or

$$4\bar{\delta}^2 - 4\bar{\delta} + (1 - \epsilon) = 0 \tag{39}$$

Where

$$\bar{\delta} = \frac{\delta}{D} \tag{40}$$

Solving above equation using almighty formula,

$$\bar{\delta} = \frac{-4 \pm \sqrt{(-4)^2 - 16(1-\epsilon)}}{8} \tag{41}$$

So that,

$$\bar{\delta} = \tfrac{1}{2}(-1 \pm \sqrt{\epsilon}) \tag{42}$$

Critical Flow Rate
The volumetric flowrate at critical-velocity is

$$Q_{cr} = v_{cr}A \tag{43}$$

According to Okafor *et al.* (2019), at critical flow, the velocity can be expressed as

$$v_{cr} = \left(\frac{Q_{cr}}{86400}\right) \cdot \left(\frac{T}{T_b}\right) \cdot \left(\frac{P_b}{P}\right) \cdot \left(\frac{z}{1.00}\right) \cdot \left(\frac{1}{A}\right) \tag{44}$$

Where
v_{cr} = critical velocity (ft/s)
Q_{cr} = critical volumetric flow rate (scfd)
T = tubing temperature (°R)
T_b = base temperature (°R)
P_b = base pressure (psia)
P = tubing pressure (psia)
z = gas compressibility factor (-)
A = tubing cross sectional area (ft²)
Substituting base temperature and pressure values of $T_b = 520$ °R and $P_b = 14.7$ psia into Equ. (44),

$$v_{cr} = \frac{Q_{cr}}{3.056 \times 10^9} \cdot \frac{Tz}{PA} \tag{45}$$

Making Q the subject,

$$Q_{cr} = 3.056 \times 10^9 \frac{v_{cr}PA}{Tz} \tag{46}$$

Liquid-loading Evaluation Method
To assess the loading status in those given wells, comparisons are carried out between current-gas flowrate (Q) and the computed critical-gas flow rate (Q_{cr}). Therefore, a gas-well is identified as:
  a) Unloading (unloaded) if the difference ΔQ of critical-gas flowrate to actual-gas flowrate is equal or less than zero ($Q_{cr}- Q \le 0$);
  b) Loading-up (loaded) if ΔQ is greater than zero ($\Delta Q> 0$).

From those respective results of ΔQ, the following interpretations are drawn out. The higher the calculated ΔQ, the higher the risks of liquid-loading. While the lower the ΔQ, the lower the risks of liquid-loading occurring.

The graphical representations of loading status are equally represented on graphs where the upright axis represents the computed critical-gas flowrate and the horizontal axis depicts theactual gas flow rate. From the graph, the data points representing the unloading gas-wells are located below the datum line (45° line) for accurate predictions. For the data points representing loading gas-wells, they appear above the 45° line. If any data points fall on datum

line or touches it, the corresponding gas-well will soon experience loading if no solutions are employed to counter or mitigate it.

As for the dots plotted on the graph representing the loading wells, correct predictions should locate them below the datum line. For any dots positioned below the datum line and touching it, loading phenomenon has just begun on those wells, and an immediate action using any Liquid-loading intervention methods on those wells will eliminate the loading phenomenon and the wells will produce again at a high-rate for long.

Liquid-loading Data Set

To authenticate the new model on vertical gas wells, data from 18 vertical gas wells from the Xinjiang North-West gas field was used. Among the data obtained from gas-field, we listed 12 gas-wells as having a low gas-liquid ratio, and 6 gas wells as having high gas-liquid ratio properties. Wellhead pressures and wellbore pressures range, respectively, from 3 MPa to 27.2 MPa, and from 16.1 MPa to 43.6 MPa. The depth of each well varies from 4359 m to 5100 m, and the tubing diameters are same for each well (62 mm). The daily gas production rate varies from 519,337.49 cfd to 5,261,885.34 cfd. From data collected, 10 gas wells are non-loading, 2 are about to load up, and 6 are loading up. Table 3.1 summarizes all the collected data.
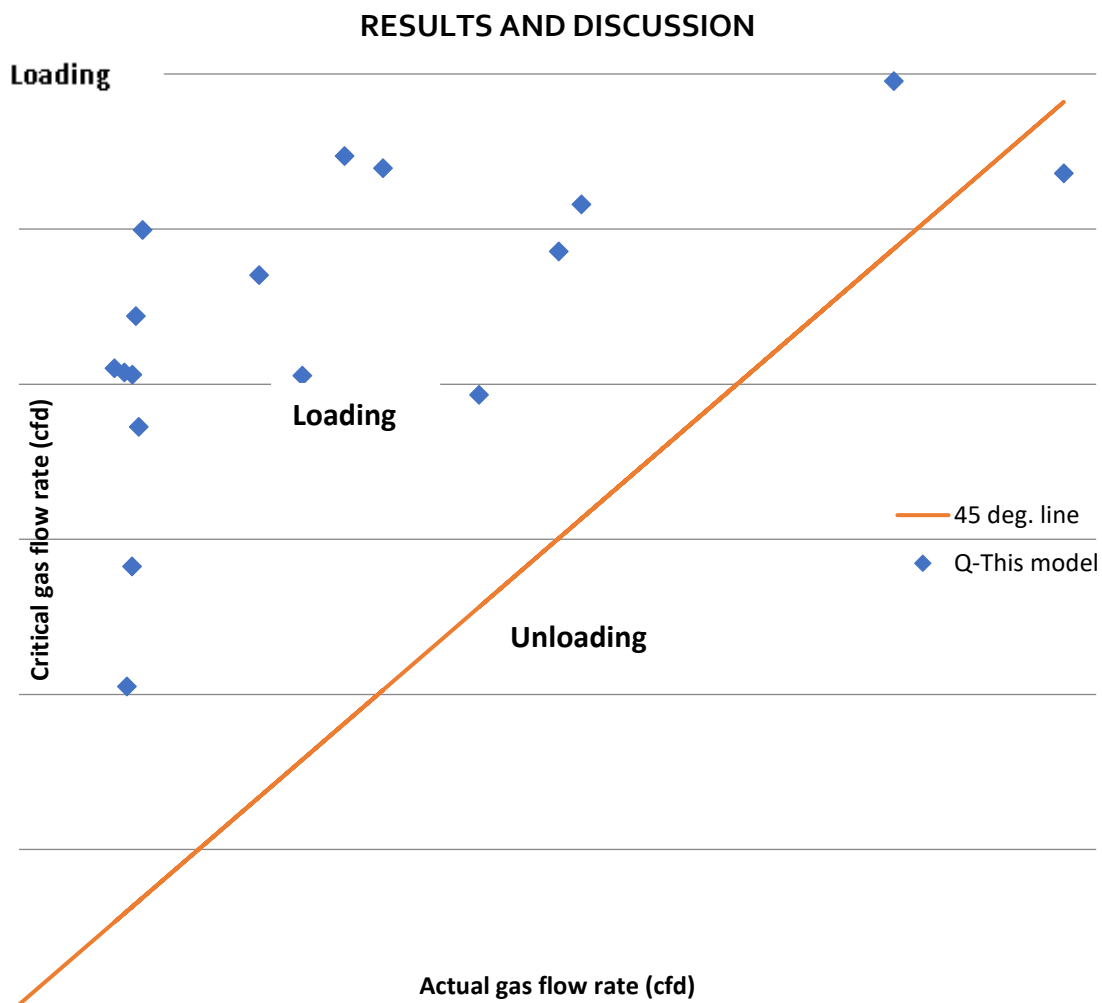
Figure 6 Developed model liquid loading prediction-results

Table 1 Summary of liquid loading predictions

Critical velocity model	Correct prediction	Wrong prediction	Prediction accuracy (%)
Turner *et al.* (1969)	12	6	66.67
Coleman *et al.* (1991)	12	6	66.67
Nossier *et al.* (2000)	16	2	88.89
Li *et al.* (2001)	11	7	61.11
Pagou and Wu (2020)	10	8	55.56
This model	7	11	38.89

Table 2 Effects of model coefficient adjustment on liquid loading prediction accuracy

| Percentage reduction (%)	Correct prediction	Wrong prediction	Prediction accuracy (%)
20	8	10	44.44
40	12	8	66.67
60	12	8	66.67
80	14	4	77.78

DISCUSSION

Figure 6 gives liquid-loading prediction-results of developed critical velocity model based on gas flowrate. From the figure, the developed model predicted status of total of seventeen (17) gas wells as loading, while one (1) well was predicted as unloading using the critical gas flowrate as the benchmark. This is different from actual gas well conditions which designated 10 wells as unloading, 6 wells as loading and two wells as about to load. In fact, on well-by-well basis, the developed model predicted correctly the actual conditions of all the loading gas wells, thereby giving it 100% prediction accuracy for the loading gas wells. The model also predicted correctly the actual conditions of one (1) of the unloading gas wells, giving it a prediction accuracy of 10% for the unloading gas wells. But the model could not accurately predict actual condition of two (2) gas wells that are about to load.
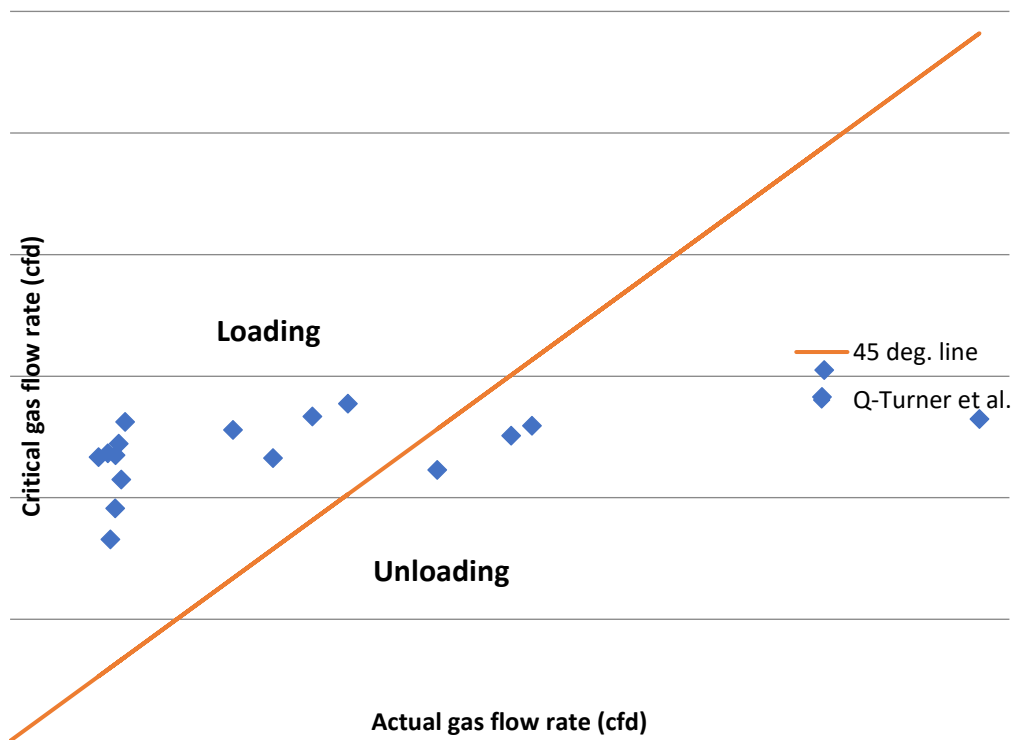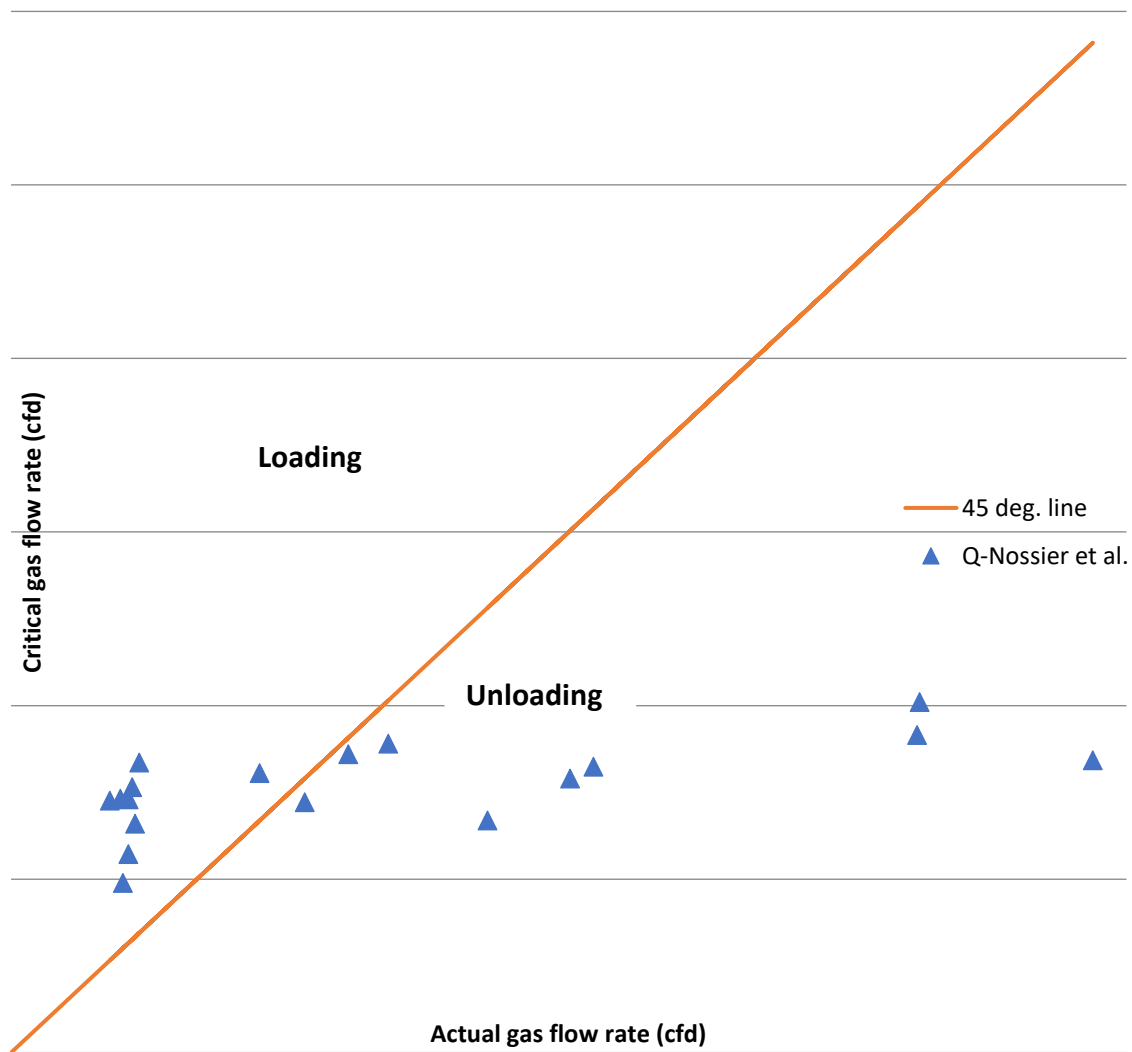
Figure 7 Turner *et al.* (1969) liquid loading prediction-results

Figure 7 gives liquid loading prediction-results of Turner *et al.* critical-velocity model based on gas flow rate. Turner *et al.* model predicted status of total of twelve (12) gas wells as loading, while six (6) wells were predicted as unloading using the critical-gas flow rate as the benchmark. This is however different from the actual gas well conditions which designated 10 wells as unloading, 6 wells as loading and two wells as about to load. In fact, on well-by-well basis, Turner *et al.* model predicted correctly the actual conditions of all the loading gas-wells, thereby giving it 100% prediction accuracy for the loading gas wells. The model also predicted correctly the actual conditions of six (6) of unloading gas wells, giving a prediction accuracy of 60 % for the unloading gas wells. But the model could not accurately predict the actual condition of the two (2) gas wells that are about to load.
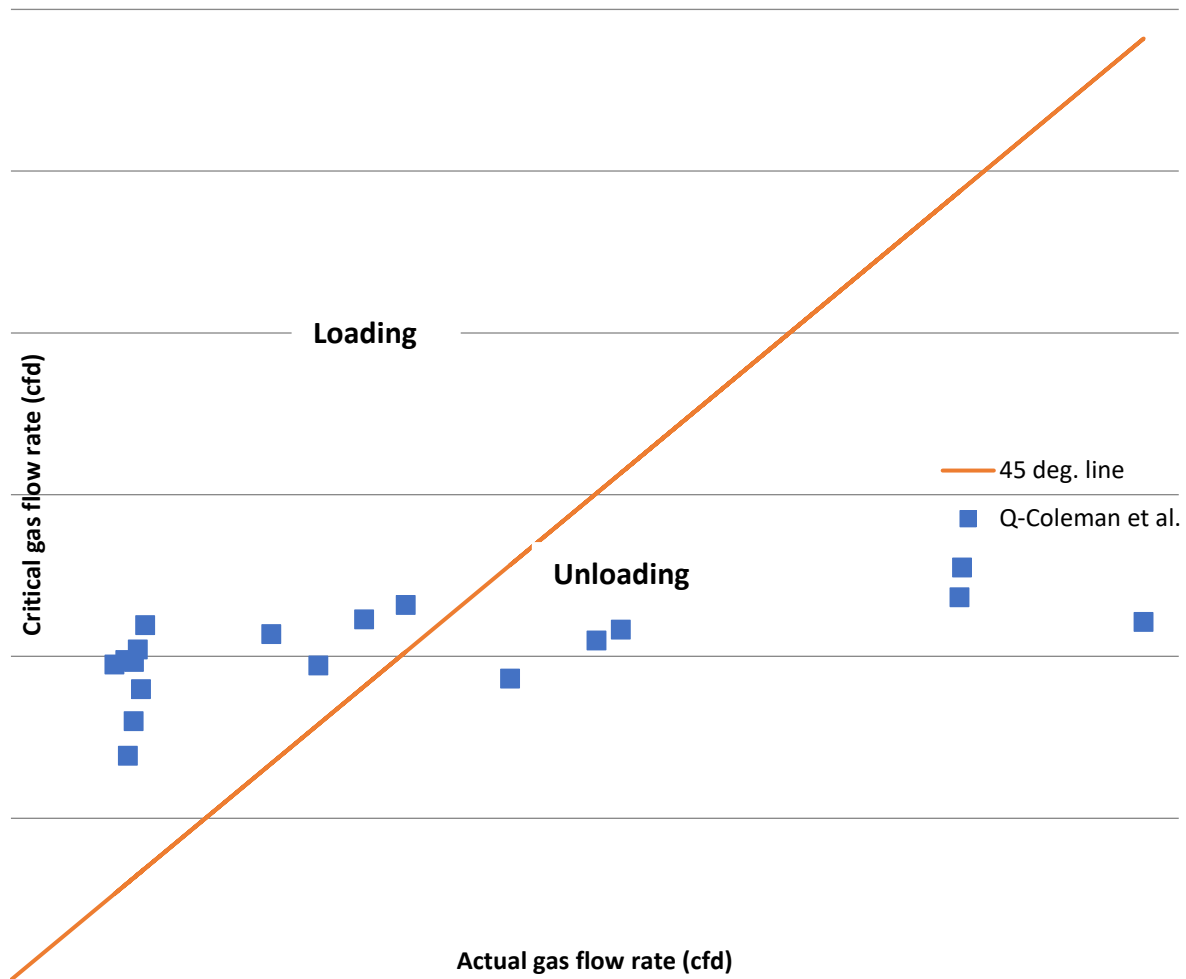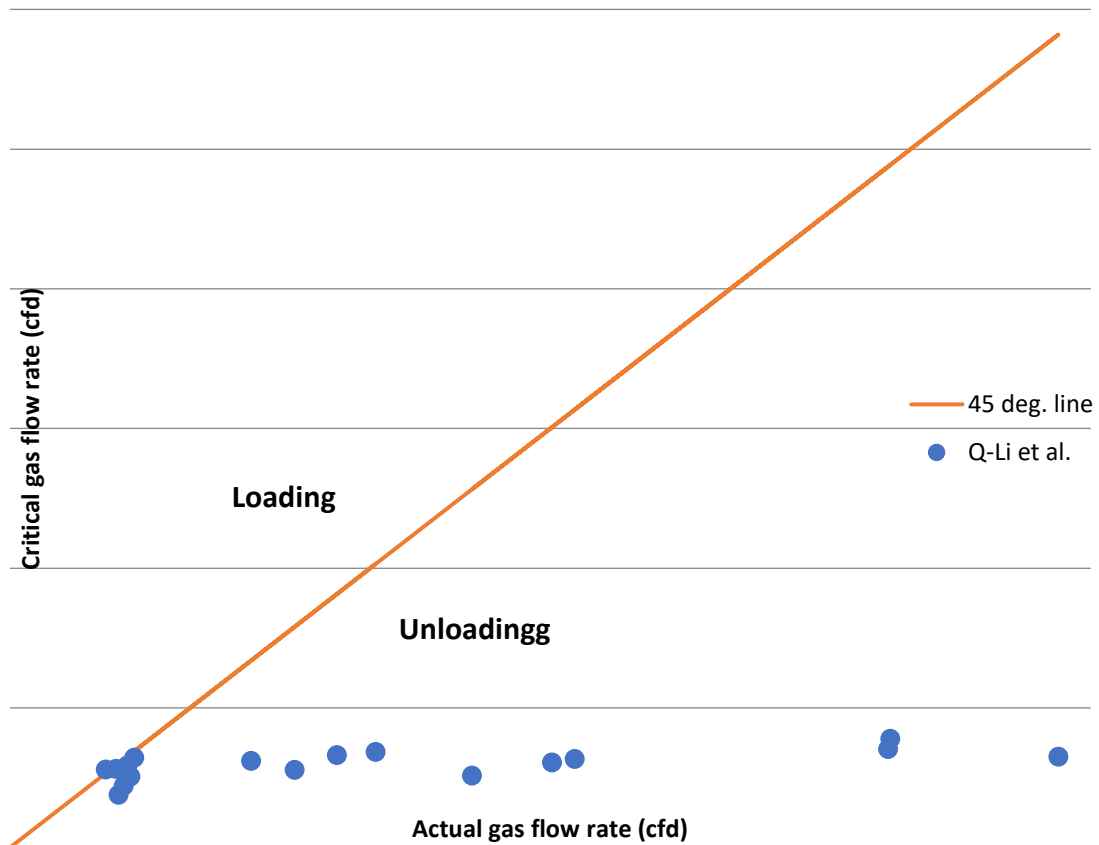
Figure 8 Coleman *et al.* (1991) liquid loading prediction results

Figure 8 gives liquid-loading prediction-results of Coleman *et al.* critical velocity model based on gas flow rate. It is clear that Coleman *et al.* model predicted the status of a total of twelve (12) gas wells as loading, while six (6) wells were predicted as unloading using the critical gas flow rate as the benchmark. This is however different from the actual gas well conditions which designated 10 wells as unloading, 6 wells as loading and two wells as about to load. In fact, on well-by-well basis, Coleman *et al.* model predicted correctly the actual conditions of all the loading gas wells, thereby giving it 100% prediction accuracy for the loading gas wells. The model also predicted correctly the actual conditions of six (6) of the unloading gas wells, giving it a prediction accuracy of 60 % for the unloading gas wells. But the model could not accurately predict the actual condition of the two (2) gas wells that are about to load.
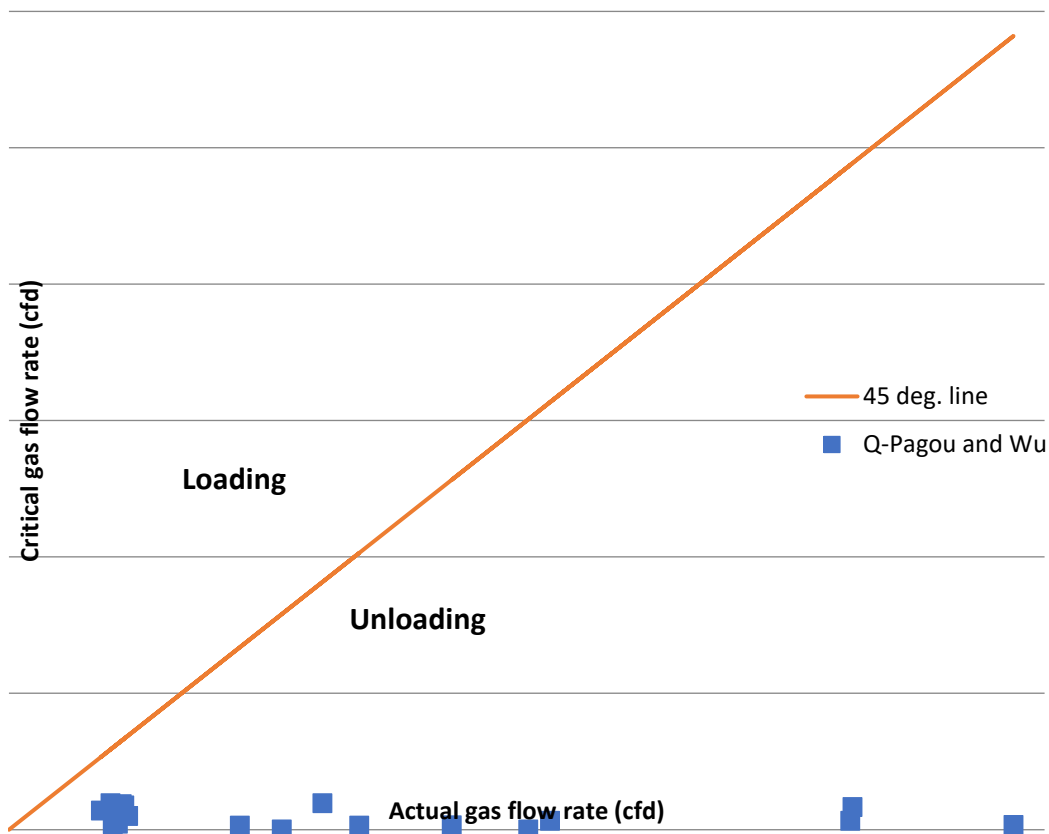
Figure 9 Nossier *et al.* (2000) liquid loading prediction results

Figure 9 gives the Liquid-loading prediction-results of Nossier *et al.* critical velocity model based on gas flow rate. Nossier *et al.* model predicted the status of a total of eight (8) gas-wells as loading, while ten (10) wells were predicted as unloading using critical-gas flowrate as the benchmark. This is however different from actual gas well conditions which designated 10 wells as unloading, 6 wells as loading and two wells as about to load. In fact, on well-by-well basis, Nossier *et al.* model predicted correctly the actual conditions of all loading gas wells, thereby giving it 100% prediction accuracy for the loading gas wells. The model also predicted correctly the actual conditions of ten (10) of the unloading gasses wells, giving a prediction accuracy of 100 % for the unloading gas wells. But the model could not accurately predict the actual condition of two (2) gas wells that are about to load.

Figure 10: Li *et al.* (2001) liquid loading prediction results

Figure 10 gives liquid-loading prediction-results of Li *et al.* critical-velocity model based on gas flowrate. Li *et al.* model predicted status of one (1) gas-well as loading, while other seventeen (17) wells were all predicted as unloading using the critical gas flow rate as the benchmark. This is however different from the actual gas well conditions which designated 10 wells as unloading, 6 wells as loading and two wells as about to load. In fact, on well-by-well basis, Li *et al.* model predicted correctly the actual conditions of one (1) of loading gas-wells, thereby giving it 20% prediction accuracy for the loading gas wells. The model also did not predict correctly actual conditions of any of the unloading gas wells, giving it a prediction accuracy of 0 % for unloading gas wells. Also, the model could not accurately predict the actual condition of two (2) gas wells that are about to load.

Figure 11: Pagou and Wu (2020) liquid loading prediction-results

Figure 11 gives the Liquid-loading prediction-results of Pagou and Wu *et al.* critical velocity model based on gas flow rate. From the figure, that Pagou and Wu *et al.* model predicted status of all eighteen (18) gas wells as unloading using critical-gas flowrate as the benchmark. This is however different from the actual gas well conditions which designated 10 wells as unloading, 6 wells as loading and two wells as about to load. In fact, on well-by-well basis, Pagou and Wu *et al.* model predicted correctly the actual conditions of all unloading gas wells, thereby giving it 100% prediction accuracy for the unloading gas wells. The model also did not correctly predict the actual conditions of all of the six (6) loading gas-wells, giving it a prediction-accuracy of 0 % for the loading gas wells. Also, the model could not accurately predict the actual condition of two (2) gas wells that are about to load.

Table 1 gives the summary of overall liquid-loading predictions by critical-velocity model's understudy. The table was generated by combining the prediction accuracies for all the categories of well status for each critical velocity model respectively. From the table, Nossier *et al.* critical velocity model gave highest prediction-accuracy of 88.89%. Also, Turner *et al.* and Coleman *et al.* models gave the same overall prediction accuracies of 66.67% respectively. The reason for this is not far from fact that both critical-velocity models were developed based on entrained-droplet model of liquid-loading (Pagou and Wu, 2020).

The next best ranked critical-velocity model was the model by Li *et al.* with an overall prediction accuracy of 61.11%. While the critical velocity model with lowest overall prediction accuracy was the developed model, which had the prediction accuracy of 38.89%. This low prediction accuracy can be explained by fact the data set used were derived from vertical wells and may not be

suitable for a critical velocity model that considers inclination angle like the one developed here (Pagou and Wu, 2020).

Table 2 gives effects of model-coefficient adjustment on liquid-loading prediction-accuracy, which was generated from Tables A13-A16. The model coefficient-adjustment was carried out following usual the work of Wolu *et al.* (2019), in which they considered the effect of model-coefficient adjustment on liquid-loading prediction-accuracies of critical-velocity models.

Model coefficient reduction was chosen because critical-velocity prediction by the developed model was higher than actual gas-velocities. It can also be deduced that model-coefficient reduction is directly proportional to liquid-loading prediction-accuracy.

Hence, by reducing model-coefficient by 20%, model prediction accuracy was increased to 44%. While model coefficient reduction by 40% further increased prediction-accuracy to 66.67%, further reduction by 60% didn't affect prediction-accuracy. But when model-coefficient was reduced further by 80%, prediction-accuracy then increased to 77.78%.

SUMMARY

A new critical velocity model has been developed for predicting onset of liquid-loading in natural gas wells. This was done following the reverse film model, while incorporating separate pressure drops for both liquid and gaseous phases.

Also, influence of production tubing length and liquid film thickness on critical-velocity prediction was equally considered. And the final model showed production tubing length as affecting critical velocities in gas wells that is previously ignored in other critical velocity models. From the model, it was deduced that the critical velocity varies directly as the square root of the tubing height. This means that as the tubing height increases, the critical velocity would equally be expected to increase, although not in a similar way.

A comparative analysis of prediction accuracy of developed-model was also conducted alongside other critical velocity models like Turner *et al.* (1969), Coleman *et al.* (1991), Nossier *et al.* (2000), Li *et al.* (2001), and Pagou and Wu (2020) models using literature data.

The obtained field data was from 18 vertical gas wells from the Xinjiang North-West gas field in China. The prediction accuracies of critical-velocity models followed the order, Nossier *et al.* (2000), Turner *et al.* (1969), Coleman *et al.* (1991), Li *et al.* (2001), Pagou and Wu (2020), and developed-model. This can probably be attributed to dearth of suitable field data sets in literature that includes production tubing height as a parameter.

To increase the prediction accuracy of developed-model, model coefficient adjustments were carried out by percentage reduction of developed model coefficient. This was done following common practice in literature where percentage adjustments are frequently made to critical velocity model coefficients to increase their liquid-loading prediction-accuracies.

In the end, the prediction accuracy of developed-model was tremendously increased by reducing model coefficient.

CONCLUSIONS

From this study, following conclusions are drawn

a) A new critical velocity model was developed for predicting onset of Liquid-loading in natural gas wells, which incorporated tubing height and separate pressure drops for both phases as parameters.

b) The developed critical velocity model was able to correctly predict liquid-loading status of some wells whose field-data were found in literature.

c) Model coefficient adjustments in the form of percentage reduction can substantially increase prediction-accuracy of developed critical-velocity models like percentage increment.

REFERENCES

Aboutaleb, G. J. G. and Vahid, K. (2015). Prediction of gas critical flow rate for continuous lifting of liquids from gas wells using comparative neural fuzzy inference system. *Journal of Applied Environmental and Biological Sciences*, *5*(8S), 196-202.

Adaze, E., Badr, H. M., and Al-Sarkhi, A. (2019). CFD modeling of two-phase annular flow toward the onset of liquid film reversal in a vertical pipe. *Journal of Petroleum Science and Engineering, 176*, 755-774

Ajani, A., Kelkar, M., Sarica, C., and Pereyra, E. (2016). Foam flow in vertical gas wells under liquid loading: Critical velocity and pressure drop prediction. *International Journal of Multiphase Flow, 87*, 124-135

Alamu, M. B. (2012). Gas-well liquid loading probed with advanced instrumentation. *SPE Journal, 17*(01), 251–270. doi: 10.2118/153724-PA.

Ali, A. J, Scott, S. L. and Fehn, B. (2003). Investigation of a New Tool to Unload Liquids from Stripper Gas Wells, SPE 84136, Presented at SPE Annual Technical Conference and Exhibition held at Denver

Alsaadi, Y. (2013). Liquid loading in highly deviated gas wells. Master's Thesis, University of Tulsa.

Arachman, F., Alkouh, A., and Wattenbarger, R. A. (2012). Bias in Rate-Transient Analysis Methods: Shale Gas Wells, SPE 159710, presented at the SPE Annual Technical Conference and Exhibition held at San Antonio, Texas, USA.

Ardhi, H. L. (2016). Modelling two phase pipe flow in liquid loading gas wells using the concept of characteristic velocity, submitted to Texas A & M University, August 2016.

Ayala, L. F. (2001). A unified two-fluid model for multiphase flow in natural gas pipelines. [Masters Dissertation], The Pennsylvania State University.

Baker, O. (1953). Design of pipelines for the simultaneous flow of oil and gas. *Oil and Gas Journal*, *53*, 185.

Barnea, D. (1986). Transition from annular flow and from dispersed bubble flow-unified models for the whole range of pipe inclinations. *International Journal of Multiphase Flow, 12*(5), 553–744. doi: 10.1016/0301-9322(86)90048-0.

Barnea, D. (1987). A unified model for predicting flow-pattern transitions for the whole range of pipe inclinations. *International Journal of Multiphase Flow, 13*(1), 1–12. doi: 10.1016/0301-9322(87)90002-4.

Barnea, D., Shoham, O., and Taitel, Y. (1982). Flow pattern transition for downward inclined two-phase flow; horizontal to vertical. *Chemical Engineering Science, 37*, 735-740.

Beggs, J. P., and Brill, H. D. (1973). A study of two-phase flow in inclined pipelines. *Journal of Petroleum Technology*, 607-617.

Belfroid, S. P. C, Schiferli, W., Alberts, G. J. N., Veeken, C. A. M. and Biezen, E. (2008). Prediction Onset and Dynamic Behaviour of Liquid Loading Gas Wells SPE 115567, presented at the SPE Annual Technical Conference and Exhibition held in Denver, Colorado, USA.

Bello, K. O. and Idigbe, K. I. (2015). Development of a new drag coefficient gas multiphase fluid systems. *Nigerian Journal of Technology*, *34*(2), 280 – 285. http://dx.doi.org/10.4314/njt.v34i2.10

Bolujo, E. O., Fadairo, A. S., Ako, C. T., Orodu, D. O., Omodara, O. J. and Emetere, M. E. (2017). A new model for predicting liquid loading in multiphase gas wells. *International Journal of Applied Engineering Research,* 12, 4578-4586

Brauner, N. (2001). The prediction of dispersed flow boundaries in liquid-liquid and gas-liquid systems. *International Journal of Multiphase Flow*, *27*, 885-910.

Brodkey, R. S. (1967). The phenomena of fluid motions, Addison-Wesley Publishing: Reading, MA.

Chen, X., Cai, X., and Brill, J. P. (1997). Gas-liquid stratified wavy flow in horizontal pipelines, journal of energy resources technology. *Transactions of the ASME*, *119*(4), 209-216.

Chen, D., Ya, Y., Gang F., Hongxia, M., and Shuangxi, X. (2016). A new model for predicting liquid loading indeviated gas wells. *Journal of Natural Gas Science and Engineering,* 34, 178–184. doi: 10.1016/jjngse.2016.06.063.

Cheng, N. (2009). Comparison of formulas for drag coefficient and settling velocity of spherical particles. *Powder Technology*, 189, 395-398

Chongyang, X., Heng, F., Leli, C., and Wenyu, P. (2021). Prediction of critical liquid loading time for water-producing gas wells: Effect of liquid drop rotation. *Journal of Petroleum Exploration and Production Technology.* https://doi.org/10.1007/s13202-021-01417-6

Chupin, G., Hu, B., Haugset, T. and Claudel, M. (2007), Integrated Wellbore/Reservoir Model Predicts Flow Transient in Liquid Loading Gas Wells, paper SPE 110461 presented at the SPE Annual Technical Conference and Exhibition, Anaheim, California,11-14 November 2007.

Cioncolini, A., and Thome, J. R. (2012). Void fraction prediction in annular two-phase flow. *Int. J. Multiphase Flow*, *43* (0), 72-84.

Coleman, S. B., Clay, H. B., Mccurday, D.G. and Norris III, L. H. (1991). A new look at predicting gas-well load-up. *Journal of Petroleum Technology, 43*(03), 329–333. doi: 10.2118/20280-PA.

Coskuner, G. and Strocen, T. (2002). Production optimization of liquid loading gas condensate wells: A case study, Paper 2002-107, presented at the Canadian International Petroleum Conference, Calgary, Alberta, Canada.

Daas, M., Golczynski, T., and Harry, J. (2012). Minimum flowrate to unload gas wells: Dynamic multiphase modeling to validate existing correlations. Paper presented at the SPE Latin America and Caribbean Petroleum Engineering Conference, Mexico City, Mexico, April 2012. Paper Number: SPE-152597-MS

Dotson, B. and Nunez-Paclibon, S. (2007). Gas well liquid loading from the power perspective, SPE 110357, presented at the SPE Annual Technical Conference and Exhibition held in Anaheim, California, USA.

Dousi, N., Veeken, C. A. M., and Currie, P. K. (2005). Numerical and analytical modeling of the gas-well liquid-loading process. (English). *SPE Prod & Oper, 21*(4), 475-482. SPE-95282-PA. http://dx.doi.org/10.2118/95282-pa.

Dukler, A. E. (1960). Fluid mechanics and heat transfer in vertical falling-film systems. *Chem. Eng. Prog. Symp. Ser.,* *56*(30), 1-10.

Duns Jr., H. and Ros, N. C. J. (1963). Vertical flow of gas and liquid mixtures in wells. Paper presented at the 6th World Petroleum Congress, Frankfurt, 19-26 June.

El Fadili, Y., and Shah, S. (2017). A new model for predicting critical gas rate in horizontal and deviated wells. *Journal of Petroleum Science and Engineering, 150*, 154–161. doi: 10.1016/j.petrol.2016.11.038

Fadairo, A., Falode, O., and Nwosu, C. S. (2015). A new model for predicting liquid loading in a gas well. *Journal of Natural Gas Science and Engineering, 26* (2015), 1530-1541

Fan, Y., Eduardo, P., and Cem, S. (2018). Onset of liquid-film reversal in upward-inclined pipes. *SPE Journal, 23*(05), 1630–1647. doi: 10.2118/191120-PA.

Falcone, G. and Barbosa, J.R. (2013). State-of-the-art review of liquid loading in gas wells, DGMK / ÖGEW Spring Conference 2013, Section Exploration and Extraction, Celle.

Fiedler, S., and Auracher, H. (2004). Experimental and theoretical investigation of reflux condensation in an inclinedsmall diameter tube. *International Journal of Heat and Mass Transfer, 47*(19), 4031–4043. doi: 10.1016/j.ijheatmasstransfer.2004.06.005.

Fore, L. B., Beus, S. G., and Bauer, R. C. (2000). Interfacial friction in gas-liquid annular flow. analogies tofull and transition roughness. *International Journal of Multiphase Flow, 26*(11), 1755–1769. doi: 10.1016/S0301-9322(99)00114-7.

Ghadam, A. G. and Kamali, V. (2015): Prediction of gas critical flow rate for continuous lifting of liquids from gas wells using comparative neural fuzzy inference system, *Journal of Applied Environmental and Biological Sciences*, *5*(8S), 196-202

Girija, E. G., Christiansen, R. L, and Miller, M. G. (2007). Experimental study of critical flow rates in the tubing-casing annulus of natural-gas wells. SPE Annual Technical Conference and Exhibition. Society of Petroleum Engineers. SPE-109609-MS.

Govier, G.W. and Aziz, K., (1972). *The flow of complex mixtures in pipes*, 4th ed. Malabar Florida: Robert E. Krieger Publishing Company.

Griffith, P. and Wallis, G. B. (1961). Two-phase slug flow. *J. Heat Transfer, ASME, 83*(3) 307-320
Grolman, E. and Fortuin, J.M.H. (1997). Gas-liquid flow in slightly inclined pipes. *Chemical Engineering Science, 52*(24), 4461-4471.

Guner, M. (2012). Liquid loading of gas wells with deviation from 0° to 45°. Master's Degree Master's Degree, University of Tulsa.

Gunner, M. (2012). An experimental study of low liquid loading in inclined pipes from 90° to 45°. Presented at the SPE Production and Operations Symposium, Oklahoma City, Oklahoma, USA 1-5 March. SPE-173631-MS. http://dx.doi.org/10.2118/173631-MS.

Guo, B., Ghalambor, A. and Xu, C. (2005). A systematic approach to predicting liquid loading in gas wells, SPE 94081, presented at the SPE Production Operations Symposium, Oklahoma City, Oklahoma, USA.

Guo, B., Ghalambor, A., and Xu, C. (2006). A systematic approach to predicting liquid loading in gas wells (English). *SPE Prod & Oper*, *21*(1), 81-88. SPE-94081- PA. http://dx.doi.org/10.2118/94081 -pa.

Hearn, W. (2010). Gas well deliquifaction, SPE 138672, Presented at the Abu Dhabi International Petroleum Exhibition & Conference, held in Abu Dhabi, UAE.

Heng, L., Shenghan, C., Zhanqing, Q., and Qi, Z., (2006). Hydraulic system designing of esp downhole gas water separation system, Paper 2006-54, Presented at the Petroleum Society's 7th Canadian International Petroleum Conference, Calgary, Alberta, Canada.

Hewitt, G. F. (1961). Analysis of annular two-phase flow: Application of the Dukler analysis to vertical upward flow in a tube, *Atomic Energy Research Establishment*, Harwell, Berkshire.

Hewitt, G. F. (2012). Churn and wispy annular flow regimes in vertical gas–liquid flows. *Energy & Fuels, 26*(7), 4067-4077. http://dx.doi.org/10.1021/ef3002422.

Hewitt, G. F., and Nicholls, B. (1969). Film thickness measurements in annular two-phase flow using a fluorescence spectrometer technique. *UICAEA Report AERE* 4506:1969.

Hinze, J. O. (1955). Fundamentals of the hydrodynamic mechanism of splitting in dispersion processes. *AIChE Journal, 1*(3), 289–295. doi: 10.1002/aic.690010303.

Ikoku, C. U. (1992). *Natural gas reservoir engineering*. Malabar, Florida: Krieger Publishing

Jiang, Y. and Rezkallah, K. S. (1993). A study on void fraction in vertical co-current upward and downward two-phase gas-liquid flow—i: Experimental results, *Chemical Engineering Communications*, *126*(1), 221-243, DOI: 10.1080/00986449308936220

Joseph, A. and Ajienka, J. A. (2010). A review of water shut-off treatment strategies in oil fields. SPE 136969, Paper presented at NAICE Tinapa-Calabar Nigeria.

Joseph, A., Ajienka, J. A., and Ukaeju, D. I. (2011). The effect of temperature on the rheology of waxy crude/non-waxy crude oil blends, *International Journal of Engineering Science*, *3* (3), 2011.pp 108-127.

Joseph, A., and Hicks, P. D. (2018). Modelling mist flow for investigating liquid loading in gas wells, *Journal of Petroleum Science and Engineering* doi: 10.1016/j.petrol.2018.06.023.

Ke, W., Hou, L., Wang, L., Niu, J., and Xu, J. (2021). Research on critical liquid-carrying model in wellbore and laboratory experimental verification. *Processes* 2021, *9*, 923. https://doi.org/10.3390/pr9060923

Khor, S. H. (1998). Three-phase liquid-liquid-gas stratified flow in pipelines. [Ph. D. Thesis], Imperial College of Science, Technology and Medicine, London.

Kumar, N. (2005). Improvements for flow correlations for gas wells experiencing liquid loading, SPE 92049, presented at SPE Western Regional Meeting held in Irvin, CA USA

Lea Jr., J. F. and Tighe, R. E. (1983). Gas well operation with liquid production, SPE11583, presented at the Production Operation Symposium held in Oklahoma, USA.

Lea, F. J. and Nickens, V. H (2004). Solving gas-well liquid-loading problems, SPE 72092, Distinguished author's Series.

Lea, J. F., Nickens, H. V. and Wells, M. (2003). *Gas well deliquification - solution to gas well liquid   loading problems*. Houston, Texas: Gulf Professional Publishing (Reprint).

Li, H., Yang, D. and Zhang, Q. (2007). A theoretical model for optimizing surfactant usage in a gas well dewatering process, Paper 2007-118 presented at the Petroleum Society's 8th Canadian International Petroleum Conference, Calgary, Alberta, Canada.

Li, J., Almudairis, F., and Zhang, H.Q. (2014). Prediction of critical gas velocity of liquid unloading for entire well deviation. Presented at the International Petroleum Technology Conference, Kuala Lumpur, Malaysia. 10-12 December. IPTC- 17846-MS. http://dx.doi.org/10.2523/IPTC-17846-MS.

Li, M., Sun, L, and Li, S (2001). New view on continuous-removal liquids from gas wells, SPE 70016, presented at the SPE Permian Basin Oil and Gas Recovery Conference held in Midland, Texas, USA.

Liu, L. (2014). The phenomenon of negative frictional pressure drops in vertical two-phase flow. *Int. J. Heat Fluid Flow*, *45*(1), 72-80. http://dx.doi.org/10.1016/j.ijheatfluidflow.2013.12.003.

Liu, Y., Chengcheng, L., Liehui, Z., Zhongbo, L., Chunyu, X., and Pengbo, W. (2018). Experimental and modeling studies on the prediction of liquid loading onset in gas wells. *Journal of Natural Gas Science and Engineering, 57,* 349–358. doi: 10.1016/ijngse.2018.07.023.

Luo, S., Kelkar, M., and Pereyra, E. (2014). A new comprehensive model for predicting liquid loading in gas wells. *SPE Prod & Oper, 29*(4), 337-349. SPE-172501- PA. http://dx.doi.org/10.2118/172501-PA.

Malin, M. (2019). An investigation into the mechanisms of liquid loading in small-diameter vertical pipes. [Masters Dissertation], Montana Tech Graduate School

Mandhane, J.M., Gregory, G.A., and Aziz, K. (1974). A flow pattern map for gas-liquid flow in horizontal pipes. *International Journal of Multiphase Flow, 1, 537-553.*

Meng, W., Chen, X.T., Kouba, G.E., Sarica, C., and Brill, J.P. (1999). Experimental study of low liquid loading gas-liquid flow in near horizontal pipes. SPE Paper 56466 presented at the SPE Annual Technical Conference and Exhibition held in Houston, TX, October.

Ming, R. and He, H. (2017). A new approach for accurate prediction of liquid loading ofdirectional gas wells in transition flow or turbulent flow. *Hindawi Journal of Chemistry*, Volume 2017, Article ID 4969765, 9 pages, https://doi.org/10.1155/2017/4969765

Nennie, E. D., Alberts, G. J. N., Belfroid, S. P. C., Peters, E., and Joosten, G. J. P. (2007). An investigation into the need of a dynamic coupled well-reservoir simulator, paper SPE 110316 presented at the SPE Annual Conference and Exhibition, Anaheim, California,11-14 November 2007.

Neves, T. R. and Brimhall, R. M. (1989). Elimination of liquid loading in low-productivity gas wells, paper SPE 18833 presented at the SPE Production Operations Symposium, Oklahoma City, OK, March 13-14.

Nosseir, M. A., Darwich, T. A., Sayyouh, M. H., and El Sallaly, M. (2000). A new approach for accurate prediction of loading in gas wells under different flowing conditions. *SPE Prod & Oper*, *15*(4), 241 -246. SPE-66540-PA. http://dx.doi.org/10.2118/66540-PA.

Oudeman, P. (1990). Improved prediction of wet-gas-well performance, SPE 19103, 18 SPE 167603 presented at the SPE Gas Technology Symposium held in Dallas.

Okafor, N. A., Aimikhe, V.J., and Kinigoma, B. (2019). Modelling the effect of acceleration term on total pressure drop in horizontal gas pipelines. *Petroleum and Coal, 61*(6), 1314-1320

Okoro, E.E., Bassey, C.I., Sanni, S.E., Ashiq, M.G.B., and Mamudu, A.O. (2019). Application of non-uniform film thickness concept in predicting deviated gas wells liquid loading. *MethodsX , 6*, 2443–2454.

Orkiszewski, J. (1967). Predicting two-. phase pressure drops in vertical pipe. *J. Petroleum*